

國立臺灣大學醫學院醫學檢驗暨生物技術學所

博士論文

Graduate Institute of Clinical Laboratory Sciences and

Medical Biotechnology

College of Medicine

National Taiwan University

Doctoral Dissertation

肺腺癌中致癌基因 miRNA-10a*和 YAP1 在轉移過程
及腫瘤生成過程之機制探討

The Mechanism of Oncogenic miRNA-10a* and YAP1 in
Metastasis and Tumorigenesis in Lung Adenocarcinoma

徐彬嚴

Pin-Yen Hsu

指導教授：俞松良 教授

Advisor: Sung-Liang Yu, Ph. D.

中華民國一百零五年七月

July, 2016

口試委員審定書



國立臺灣大學博士學位論文

口試委員會審定書

肺腺癌中致癌基因 miRNA-10a* 和 YAP1 在轉移過程
及腫瘤生成過程之機制探討

**The Mechanism of Oncogenic miRNA-10a* and
YAP1 in Metastasis and Tumorigenesis in Lung
Adenocarcinoma**

本論文係徐彬嚴君（學號 D98424007）在國立臺灣大學
醫學檢驗暨生物技術學研究所完成之博士學位論文，於民國
105 年 07 月 26 日承下列考試委員審查通過及口試及格，特
此證明

口試委員：

俞松良

（簽名）

（指導教授）

潘昌利

黃國毅

董國衡

楊萬華

陳玉山

系主任、所長

林立吉

（簽名）

謝誌



首先，我要感謝我的指導教授俞松良老師，回想九年前從我當研究助理開始到現在完成博士班學位，一路上老師總是用正面積極的態度指引我走向正確的方向，求學過程中我們總是自主學習，由於老師本身事務繁忙，但總是不吝惜撥空甚至熬夜和我討論實驗進度和解決問題，此外，老師也認真教導我論文撰寫的技巧，這些年的訓練也讓我能擁有獨立完成實驗的能力。同時我也要感謝口試委員：周玉山老師、楊慕華老師、蘇剛毅老師、華國泰老師和潘思樺老師在百忙之中抽空參加口試，並且給予許多珍貴的指導以及對未來研究方向提供相當豐富的建議。另外，我要感謝楊泮池校長對於我實驗研究上的建議和指教，由於校長本身無論在臨床上和生醫實驗上都有著深厚的基礎，所以我們研究生們有幸能在校長實驗室裡面學習最新的研究概念和嚴謹的實驗設計。

另外，最感謝的是何炳慶博士，學習並討論不少分生實驗技術。還有感謝台北病理中心顧文輝主任，感謝您熱情大力地協助我們 IHC 的判讀。最後感謝台大基因體中心 NGS 實驗室和微陣列實驗室的學長姐、學弟妹和助理們在生活或實驗上的協助。

感謝我可愛的家人們，你們總是默默地支持我、關心我還有包容我。還有高中大學的好友們，謝謝你們時常和我分享生活上的資訊，畢竟幾乎犧牲每個週末以及整天待在實驗室較容易和社會脫節，也讓我價值觀沒有因而偏差扭曲。

這段漫長的旅程，就像人生的縮影，這幾年內經歷了許多悲歡離合，曾經被我傷害過的人我深感抱歉，反之，對於傷害我的人我也因此而成長，路遙知馬力日久見人心，我們從不需要浪費太多寶貴的時間去證明別人的誤解，充實地每天持續進步成長才算是對自己負責。

中文摘要



越來越多的證據指出小分子核糖核酸在癌症形成的形成與侵襲過程中扮演重要的角色。經由我們將十六個肺腺癌細胞株各自所有的小分子核糖核酸 (miRNA) 表現以及細胞本身侵襲能力綜合比較之後，發現六個和細胞侵襲能力相關的 miRNA，接者，藉由一個包含九十八個肺腺癌病人的臨床試驗我們發現 miR-10a* 是一個以細胞侵襲能力為依據的預後指標基因。另外，我們是目前第一個驗證組蛋白去乙醯酶 5 (HDAC5) 是 miR-10a* 的直接目標物。HDAC5 可能是藉由抑制轉錄因子 AP-1 的表現來達到負向調控基質金屬蛋白酵素-2 和基質金屬蛋白酵素-9 的表現。此外，我們讓細胞過度表現 miR-10a* 之後可以藉由其基因微陣列晶片結果發現排名第四名的訊息路徑是和 YAP 相關，我們先前研究發現在有高度家族顯性的肺腺癌中 YAP1 R331W 會是個容易罹患的對偶基因點突變，在此篇研究裡面我們發現 YAP1 R331W 本身和 WT 組別比較之後可能是藉由增加 YAP1 在細胞核內的累積量、降低 YAP1 S127 磷酸化程度、增強 YAP1-TEAD4 的相互作用和提高 YAP1 蛋白的穩定程度等多項因素來達成在動物實驗中觀察到 YAP1 R331W 具有較強的腫瘤生成能力。我們在此篇研究清楚地驗證出致癌性基因 miR-10a* 和 YAP1 在肺腺癌中的致癌機制。

關鍵字：轉移、致癌性小分子核糖核酸、組蛋白去乙醯酶 5、Hippo 訊息傳遞路徑、YAP1 絲胺酸 127

Abstract



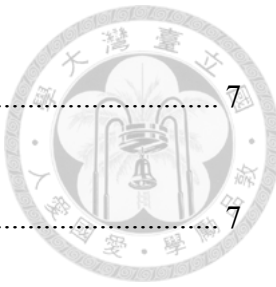
The growing evidences implied that miRNAs play important roles in different states of cancers as well as cancer invasion. Comparison between the miRNA expression profiles and the invasiveness of 16 lung adenocarcinoma cells, 6 invasion-related miRNAs were found. Using a cohort of 98-lung adenocarcinoma patients, we identified miR-10a* is an invasion-based prognostic gene in lung adenocarcinoma. Besides, we firstly found that histone deacetylases 5 (HDAC5) is a direct target of miR-10a* and it also is important for miR-10a*-promoted invasiveness. HDAC5 might down-regulate MMP-2 and MMP-9 expression through down-regulation of transcription factor AP-1. Besides, YAP signaling pathway was ranked number 4 of the array result of miR-10a* overexpressing cells. Before, we identified that YAP1 R331W is an allele predisposed for lung adenocarcinoma with high familial penetrance. We found YAP1 R331W might increase tumorigenesis *in vitro* and *in vivo* through higher YAP1 nuclear accumulation, lower phosphorylation of YAP1 Ser127, stronger YAP1-TEAD4 interaction and better protein stability than WT group. We clearly demonstrated the mechanism of oncogenic miRNA-10a* and YAP1 in metastasis and tumorigenesis in lung adenocarcinoma.

Keyword : Metastasis, oncogenic miRNA, HDAC5, Hippo pathway, YAP1 Ser127

Content



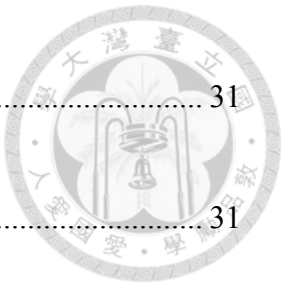
□試委員審定書	I
謝誌	I
中文摘要	II
Abstract	III
List of Figures	VIII
List of Tables	XI
Introduction	1
Metastasis	1
Lung cancer	1
MiRNAs and tumor metastasis	2
HDACs and cancer	3
Driver mutations in cancer	4
Hippo signaling pathway	5
Motivation and purpose	6



Materials and methods.....	7
Cell culture.....	7
Human lung adenocarcinoma patients and tumor specimens.....	7
Invasion assay	8
Real-time quantitative PCR (qRT-PCR).....	8
MicroRNA expression microarray.....	9
miRNA precursor and siRNA transfection	10
Plasmid Construction.....	11
mRNA expression microarray	12
Luciferase reporter assay	13
Western blot assays.....	13
Gelatin zymography.....	14
Immunohistochemistry Staining	15
shRNA lentivirus infection	15
Colony formation assay	16



Xenograft tumor models	16
Immunoprecipitation.....	17
Nuclear and cytoplasmic extraction.....	18
Statistical analysis.....	18
Results	19
Part-I	19
MiR-10a* expression associates with poor survival in lung adenocarcinoma.....	19
MiR-10a* promotes cell invasion <i>in vitro</i>	20
HDAC5 is a miR-10a* target.....	21
HDAC5 attenuates the invasive ability of lung adenocarcinoma cells	23
Mechanism of miR-10a*-induced invasiveness.....	25
Part-II	27
YAP1 R331W mutation increased colony formation <i>in vitro</i> and <i>in vivo</i>	27
YAP1 R331W mutation promoted invasiveness <i>in vitro</i>	29
The potential YAP1 R331W mediated-mechanisms in lung adenocarcinoma	30

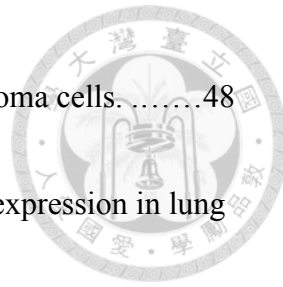


Discussion.....	31
Part-I	31
Part-II	35
References	75



List of Figures

MiR-10a* expression associates with poor survival in lung adenocarcinoma.....	38
Each of six microRNAs expression was significantly correlated to invasiveness in lung adenocarcinoma cells.	39
Patients with high miR-10a* expression were significantly correlated to poor outcome of Overall survival and Relapse survival.	40
The expression of miR-10a* showed a moderate correlation with invasiveness of 16 lung adenocarcinoma cells.	41
Inhibition of miR-10a* attenuated the invasion abilities of lung adenocarcinoma cell lines.....	42
MiR-10a* decreased endogenous protein level of HDAC5.	43
MiR-10a* significantly inhibited the protein and RNA levels of endogenous HDAC5 in lung adenocarcinoma cells.	44
MiR-10a* significantly suppressed the luciferase activity in the construct of wild-type HDAC5 3'UTR.	45
The expression of HDAC5 was negatively correlated with miR-10a* expression in lung adenocarcinoma patients.	47



Inhibition of HDAC5 enhanced the invasiveness of lung adenocarcinoma cells.....	48
MiR-10a*-mediated invasive ability was attenuated by HDAC5 overexpression in lung adenocarcinoma cells.....	49
AntagomiR-10a*-decreased invasive ability was rescued by si-HDAC5 delivery in lung adenocarcinoma cell line HOP-62.....	50
Overexpression of HDAC5 inhibits mRNA level and activity of MMP-2 and MMP-9..	51
Overexpression of HDAC5 inhibits mRNA level of c-Fos and c-Jun.....	52
Lacking of c-FOS abolished si-HDAC5-enhanced MMP-2 and MMP-9 promoter activities.....	53
MiR-10a* enhanced MMP-2 and MMP-9 mRNA expression in lung adenocarcinoma cells.....	54
MiR-10a*-induced invasive ability was attenuated by si-MMP-2 and si-MMP-9 delivery in lung adenocarcinoma cell line HOP-62.....	55
Model of miR-10a*-regulating network.....	56
Microarray result indicated that transfection of miR-10a* can increase the relative fold change of p38, MEK3 and uPA.....	57
Overexpression of YAP1 R331W mutation did not play the driving role in the	



development of tumorigenesis.	58
YAP1 R331W significantly increased the number of colonies and each area of colony <i>in vitro</i>	59
YAP1 R331W mutation increased colony formation <i>in vivo</i>	60
YAP1 R331W mutation increased relative expression level of Oct4 and Sox2 <i>in vitro</i> . 62	
YAP1 R331W mutation significantly promoted invasiveness and enhanced MMP9 mRNA in TAZ knockdown cells.	63
YAP1 R331W increased YAP1 nuclear accumulation and inhibited YAP1 S127 phosphorylation <i>in vitro</i>	64
YAP1 R331W increased YAP1-TEAD4 interaction in lung adenocarcinoma cells.....	65
YAP1 R331W enhanced YAP1 protein stability.	66

List of Tables



Primer/Probe lists of experiments	67
Six invasion-related miRNAs.....	69
Clinicopathological characteristics of 98 lung adenocarcinoma patients.....	70
Multivariate Cox regression analysis of the miR-10a* expression and survivals in 98 NSCLC patients.....	71
MiR-10a*-altered pathways.....	72
Invasion related pathways altered by HDAC5 overexpression.....	73
Potential transcription factors involved in HDAC5-mediated regulation of MMP-2 and MMP-9.....	74



Introduction

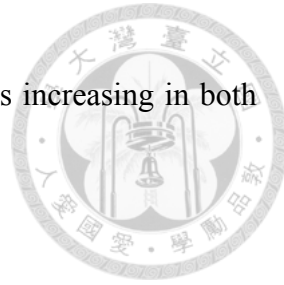
Metastasis

Cancer metastasis is a multi-step process, by which cancer cells move from a primary tumor to secondary one in distant sites. Metastasis is the key cause of mortality in cancer patients (1). For most patients, metastasis has already begun when the cancer is diagnosed (2, 3). Among all cancer types, just one in five patients diagnosed with metastatic cancer will survive more than 5 years. Only a few patients with metastatic cancer can be cured by surgery, and the effects of other treatment are limited (4). A theory supposed to explain the metastatic preference of cancer cells for specific organs is called the “seed and soil” theory. The cancer cells play the roles “seeds” and the specific organ microenvironments play the roles “soil”. The secondary tumor can be determined by the interaction between the “seeds” and the “soil” (5).

Lung cancer

Lung cancer is still the leading cause of cancer-related death in most countries. Besides, over eighty percentages of patients diagnosed with lung cancer, who also are present with metastatic disease (6). Adenocarcinoma, the most common type, around forty

percentage of all incidences of lung cancer, and its preference rate is increasing in both Asian and Western countries (7).



MiRNAs and tumor metastasis

Several lines of evidence indicate that miRNAs play important roles in different states of cancers and developmental lineage (8). MicroRNAs are small RNAs 18 to 24 nucleotides in length that serve the important regulation of genes. Instead of being translated into proteins, the mature single-stranded miRNA binds to the messenger RNAs (mRNAs) to interfere with the translational level or to induce mRNA degradation. Only around 1% of the genomic transcripts in mammalian cells encode miRNA, almost one-third of the encoded genes are regulated by miRNAs (9). In general, miRNAs play two opposing roles in the process of cancer progression, oncogenic and protective miRNA. The miR-17–92 clusters, a first identified oncogenic miRNA in mammals, is a direct effector of the c-myc oncogene and also named oncomiR-1 (10). Currently, numerous metastasis promoter and suppressor miRNAs have been clearly identified and classified (11). For example, miR-10b initiates tumor invasion and metastasis processes through targeting of the HOXD10 in breast cancer (12). However, miR-34a has been shown to inhibit metastasis through targeting of the CD44, Fra-1 and Snail in prostate cancer, breast

cancer and colorectal cancer (13-15). The important roles of miRNAs in metastasis and tumorigenesis facilitated the development of miRNA-based diagnostic and prognostic biomarkers as well as anticancer therapeutic agents. Results from several clinical trials have provided evidence to support the use of antisense miRNA to suppress oncogenic miRNA for cancer therapy (16).

HDACs and cancer

Histone deacetylases (HDACs) cause chromatin condensation and transcriptional repression by removing acetyl groups from lysine residues in histone protein (17, 18). To date, 18 identified human HDACs are grouped into classes I-IV. HDAC5, a member of the class IIa, plays a crucial role of cell differentiation and development in normal human tissues including myocardium, brain and skeletal muscle (19, 20). HDAC5 has been shown to play critical role in cardiac disease. HDAC5 has been reported to suppress myocyte enhancer factor 2 (MEF2) transcriptional activities during muscle development (21, 22). Currently, little is known about the role of HDAC5 in cancer categories. As for lung cancer, only Osada reported that reduced expression of HDAC5 and HDAC10 is associated with poor prognosis in lung cancer patients (23). Two studies reported that reduced HDAC5 expression has happened in colon cancer and acute myeloid leukemia

(24, 25). However, an upregulation of HDAC5 is associated with poor survival in high-risk medulloblastoma (26). Despite of advances in the diagnosis and therapy of cancers, the therapeutic outcome and patients' survival are not satisfied yet. Cure of the diseases by surgery is only achieved in cases representing an early stage of cancers.

Driver mutations in cancer

Next generation sequencing has identified millions of somatic mutations in cancer cells [e.g., The Cancer Genomic Atlas (TCGA), the Cancer Genome Project (CGP), and the International Cancer Genome Consortium]. However, not all mutations in cancer genomes are related to malignant initiation and progression. The major challenge is to distinguish which genetic or epigenetic changes are drivers of cancer development and it also is the critical step in developing targeted therapies (27). Oncogenes can be affected by focal amplification or missense mutation at a limited number of codons, whereas tumor suppressor genes can be affected by deletions or nonsense, frameshift, and splice-site mutations (28). For example, the BRAF oncogene is usually affected by the V600E mutation (29). The MYC oncogene in non-Hodgkin lymphoma is often through gene rearrangements (30). Interestingly, the occurrence of somatic copy number mutations (CNAs) and the occurrence of somatic single-nucleotide variants (SNVs) were

reversely correlated across 12 cancer types (31).



Hippo signaling pathway

After the discovery of YAP by Marius Sudol in 1994 (32), the biology and regulation of YAP/TAZ has been well investigated by many researchers. The transgenic mice showed that overexpression of YAP results in enlarged liver four times the size of control group and causes liver tumors (33). YAP1, a downstream effector of the Hippo pathway, plays a master regulator normal tissue homeostasis (34), differentiation and apoptosis of normal stem cells (35). YAP1 also has been demonstrated to promote tumor growth, metastasis in many solid tumors (36). The animal model indicated that YAP may cooperate with MYC oncogene to promote tumor growth (37). Several researches demonstrated that YAP1 acted as an oncogene in several cancers. We also identified the YAP1 R331W germline mutation as a high-risk factor for lung adenocarcinoma (38).



Motivation and purpose

Part-I

In our previous studies, Yu et al. discovered five risk-and protective miRNAs signatures, which can predict the survival of NSCLC patients (39). Hsu et. al. found invasion-associated four-gene signature, which were derived from lung cancer cell lines and had good survival prediction power for NSCLC patients (40). All these studies suggest us that microRNAs that can discriminate the invasion ability of cancer cells may become useful candidates for clinical outcome prediction. The aim of this study is to discover the invasion-based miRNA signature

Part-II

In our previous study, Chen et. al. found YAP1 R331W, a germline mutation, which is also an allele predisposed for lung adenocarcinoma with high familial penetrance (38). Until recently, the underlying molecular mechanism of this mutation remains unknown. The aim of this study is to investigate the molecular mechanism of YAP1 R331W in lung adenocarcinoma cells.

Materials and methods

Cell culture



11 lung adenocarcinoma cell lines (A549, EKX, HOP-62, NCI-H23, NCI-H322M, NCI-H522, H1437, H1568, H1650, H1755 and H1975) were purchased from the Developmental Therapeutics Program (DTP) of the National Cancer Institute (NCI) and American Type Culture Collection (ATCC, Manassas, VA); other five cell lines were established from Taiwanese lung adenocarcinoma patients (CL1-0, CL1-5, PE-089, VL080 and VL-107). Most cell lines were cultured in RPMI 1640 medium (Invitrogen, Taipei, Taiwan) with 10% fetal bovine serum, penicillin (100 units/ml), L-glutamine (2mM) and streptomycin (100 g/ml) at 37°C under 5% CO₂. Only CL1-0, CL1-5 and HEK293T were cultured in DMEM medium with the same condition of RPMI1640 medium.

Human lung adenocarcinoma patients and tumor specimens

A total of 98 clinical lung tumor tissue specimens were recruited from Taichung Veterans General Hospital (Taichung, Taiwan) between May 2000 and June 2009. This investigation was performed after approval by the Institutional Review Board. Written

informed consent was obtained from all patients.



Invasion assay

In vitro cell invasion assay was performed as previously described (38) using transwell chambers (8 μm pore size; Costar, Cambridge, MA). Filters were coated with Matrigel (Becton Dickinson, Franklin Lakes, NJ), and 2×10^4 HOP 62 cells or 6×10^4 H1650 cells were seeded on top of the polycarbonate filters and incubated for 16 hours. 2×10^4 A549 cells (all transiently or stably expressed clones) were seeded on top of the polycarbonate filters and incubated for 16 hours. Filters were swabbed with a cotton swab, fixed with methanol and then stained with Giemza solution (Sigma, St Louis, MO). The cells attached to the lower surface of the filter were counted under a light microscope (Magnification $\times 100$).

Real-time quantitative PCR (qRT-PCR)

Total RNA was extracted from cells by using TRIzol reagent (Invitrogen, Thermo Scientific, Carlsbad, CA), and reverse transcribed with an SSRTIII (Invitrogen), 10 ng cDNAs were used to quantify the mRNA expression of target gene by using the SYBR-Green Master PCR Mix (Thermo Fisher Scientific, Carlsbad, CA) in triplicate.

The mature form of miRNAs was quantified by using the TaqMan MicroRNA Assay Kit, according to the manufacturer's instructions (Thermo Fisher Scientific) in triplicate. The relative expression level of target gene was determined as $-\Delta CT = - [CT_{\text{target}} - CT_{\text{reference}}]$, TBP and U6 served as reference for the mRNA and microRNA assay, respectively. The target/reference RNA ratio was calculated as $2^{-\Delta CT} \times K$, in which K is a constant. All primers and probes were listed in Table 1.

MicroRNA expression microarray

The mature microRNAs of 16 lung adenocarcinoma cells were amplified from 200 ng total RNAs by the Illumina human v2 MicroRNA expression profiling kit containing primers for 1,146 human microRNAs. The resulting amplicons were hybridized to a 96 sample universal probe capture array and fluorescent signals were detected by confocal laser scanning. All steps were performed according to Illumina's instructions manual. The raw data extraction of miRNA microarrays was performed with GenomeStudio Software v2011.1. according to the manufacturer's protocol (Illumina). To focus on the functional miRNAs we only analyzed the miRbase annotated miRNAs (858 out of 1146 miRNAs). The data were treated by log2 transformation and quantile normalization using JMP software. The averaged values of each miRNA in low-invasive group and

high-invasive group were analyzed; we defined it as a risk miRNA if value of high-invasive group was greater than low-invasive one. Student T-test and FDR adjustment were our statistical analysis way. The array data was uploaded onto GEO (GSE83952).



miRNA precursor and siRNA transfection

Pre-miR-NC, Pre-miR-10a*, Anti-miR-NC and Anti-miR-10a* precursors were purchased from Ambion (Ambion, Thermo Scientific, Carlsbad, CA) which are single-stranded, chemically modified oligonucleotides and design to increase or reduce the level of endogenous miR-10a*. The cells were transfected with miRNA precursors through siPORT-Neo-FX (Ambion) transfection reagent, respectively. Forty-eight hours after transfection, cells were used for invasion assay, luciferase reporter assay and Western blot assays. The miR-10a* expression of all transfected cells was examined by qRT-PCR. Cells were transfected with si-NC and two HDAC5 siRNAs (Ambion) using lipofectamine 2000 reagent (Invitrogen, Thermo Scientific, Carlsbad, CA) with standard protocol.



Plasmid Construction

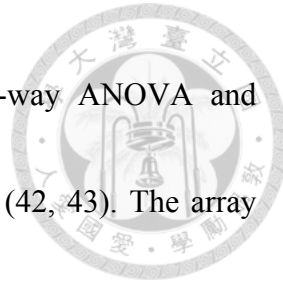
The full-length wild-type HDAC5 3'UTR was amplified from genomic DNA of lung adenocarcinoma HOP-62 cells using forward primer 3'UTR-F and the reverse primer 3'UTR-R (Table 1). Two miR-10a* binding sites of HDAC5 3'UTR were predicted by RNA22 algorithm (41). The PCR products of HDAC5 3'UTR with two mutant miR-10a* binding sites were generated by PCR-based mutagenesis method with the paired primers (Mut1F'/Mut1R', Mut2 F'/Mut 2 R' listed in Table 1. The PCR fragments were subcloned into pMIR-REPORTER luciferase vector (Invitrogen), respectively. The stem loop structure of pre-miR-10a and miR-10a sponge were generated using the primers, which were listed in Table 1. These PCR fragments were respectively subcloned into psilencer 4.1 vector (Ambion) and pcDNA3.1 (Invitrogen). The human full-length open reading frame (ORF) of HDAC5 and YAP1 were respectively generated from cDNA of lung adenocarcinoma HOP-62 and A549 cells using the primers, which were listed in Table 1. YAP1 R331W mutation fragment was generated using the primers, which were listed in Table 1. All PCR fragment was subcloned into pCMV-Tag-2A (Invitrogen). The human MMP-2 and MMP-9 promoters were generated from genomic DNA of lung adenocarcinoma HOP-62 cells using the primers, which were listed in

Table 1). PCR fragment was subcloned into pGL4.17 (Promega, Madison, WI). The accuracy of cloned sequences were validated by Sanger sequencing. All transfection experiments were performed with Lipofectamine 2000 reagents or Lipofectamine LTX (Invitrogen) in accordance with the manufacturer's protocols.

mRNA expression microarray

Expression profiling was conducted on pre-NC transfected and pre-miR10a* transfected cells and HOP-62 cells harboring HDAC5-expressing or mock vectors at the Microarray Core (NTU Center of Genomic Medicine, Taipei, Taiwan) using the DASL protocol for the Illumina HT-12 V4 BeadChip array. RNA quality was assessed using the Bioanalyzer 2100 (Agilent Technologies, Santa Clara, CA). RNA Integrity Number (RIN) ranged from 8.0 to 10.0. Target AmpTM – Nano Labeling Kit was used to transcribe 400ng total RNA according to the manufacture's protocol. 700 ng cRNAs were hybridized to the Illumina HumanHT-12 v4 Expression BeadChips (Illumina, San Diego, CA) at 58°C for 16 hours. BeadChips were scanned using an Illumina BeadArray Reader and the Bead Scan Software (Illumina). Microarray data were normalized in Partek Genomics Suite v6.6 using per-probe median-centered quantile normalization. Data analysis was conducted on log2-transformed fold change data. The differentially

expressed genes with 1.3-fold change were identified using one-way ANOVA and corrected by false discovery rate (FDR < 0.05) as previous reports (42, 43). The array data was uploaded onto GEO (GSE83952).



Luciferase reporter assay

The luciferase reporter constructs (pMIR-HDAC5 3'UTR-Wt, BS1-Mut, BS2-Mut, B1+2-Mut, MMP-2 promoter or MMP-9 promoter) along with the control plasmid (pRL-TK Vector; Promega, Madison, WI) were cotransfected into HEK293T cells by lipofectamine 2000 (Invitrogen) after HEK293T cells were seeded 24 hours prior to transfection. After 48 hours incubation the Dual-Glo luciferase substrate (Promega) was added and the luminescent signals were measured by Spectramax Paradigm multimode detection platform (Molecular Devices, Sunnyvale, CA) in triplicate. The activity of Renilla luciferase was used as an internal control to normalize transfection efficiency.

Western blot assays

Cells lysates were prepared in the RIPA buffer containing protease inhibitors (Roche, Meylan, France). The proteins were separated by 8%~12% SDS-PAGE and blotted onto nitrocellulose membrane (Millipore, Bedford, MA). Proteins were probed with the

specific specific antibodies, visualized by chemiluminescence assay kit (Merck Millipore, Temecula, CA) and detected by GE FUJI ImageQuant LAS4000 chemiluminescence imaging system (GE Healthcare Bio-Sciences Corporation, Piscataway, NJ). Primary antibodies (Abs) used for Western blot assays were as follows: anti-HDAC5 Ab (Cell signaling), anti-FLAG Ab and anti- β -actin Ab (Santa Cruz Biotechnology), β -actin acts as an internal control.

Gelatin zymography

Cells were transfected with Pre-NC control and miR-10a* mimics for 48 hour, respectively and were cultured in serum-free medium. Then the supernatants were collected after 16 hours. The supernatants were loaded into the wells of precast gels (10% polyacrylamide gels containing 0.1% gelatin). Separated gels were washed in a buffer containing 2.5% Triton and subsequently incubated in reaction buffer containing 10mM CaCl₂, 1 % NaN₃, and 40 mM Tris-HCl, pH 8.0, at 37 °Covernight. Finally, the gels were stained with0.25 % (w/v) Coomassie blue in 10 % acetic acid (v/v) and 20 % methanol (v/v) and distained in 10 % acetic acid (v/v) and 20 % methanol (v/v). The gelatinolytic activity was analyzed by the GE FUJI ImageQuant LAS4000 chemiluminescence imaging system (GE Healthcare Bio-Sciences Corporation,

Piscataway, NJ).



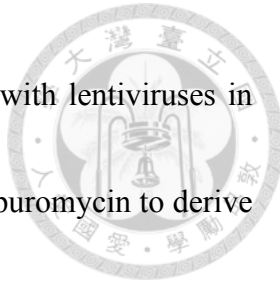
Immunohistochemistry Staining

The formalin-fixed and paraffin-embedded specimens were sectioned at a thickness of 4 μM andstained by IHC. HDAC5 IHC stainingwas performed on a VENTANA BenchMark ULTRA automated slide processing system (Ventana Medical Systems, Tucson, AZ). Inbrief, slides of NSCLC tumor were subjected to deparaffinizationusing EZ Prep (VMSI) and extended Cell Conditioning 1.Tissue sections were then incubated with anti-HDAC5 antibody (1:500, ab55403, Abcam, Cambridge, MA) for 32 minutes. OptiView DAB IHC Detection Kit (VMSI) were used. Tissue slides were counterstained with Hematoxylin II (VMSI) and Bluing Reagent (VMSI). Slides were dehydrated and cleared before cover slipping.

shRNA lentivirus infection

The lentiviral YAP1 shRNA constructs were purchased from the National RNAi Core Facility in Academia Sinica, Taiwan). Vectors expressing shRNA against human YAP1 (TRCN_107265, 5'-CCCAGTTAAATGTTCACCAAT -3') and human TAZ (TRCN_296572, 5'-TGCTTCCTCAGTTACACAAAG-3'). Both the lentiviruses production and

infection were followed by standard protocols. Cells were infected with lentiviruses in medium containing polybrene (8 μ g/ml). The cells were treated with puromycin to derive a pool of resistant shRNA clones after virus infection.

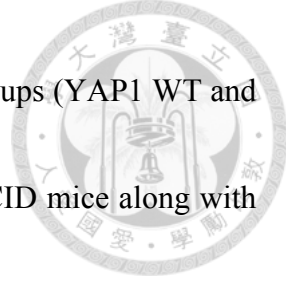


Colony formation assay

To determine the ability of cells in an anchorage-independent manner, the bottom layer of six-well plates contained 0.7% agarose in phosphate-buffered saline, and the top layer contained 0.3% agarose in medium with 10% fetal bovine serum. Cells were suspended in 1 ml RPMI-1640 containing 0.35% low-melting-point agarose and were seeded onto the top layer at density of 2×10^3 cells per well. After 3-4 weeks, the wells were washed in PBS, fixed in 4% paraformaldehyde, and stained with 0.1% crystal violet. Colonies greater than 0.5 mm were counted in three independent experiments.

Xenograft tumor models

Age-matched 6weeks NOD/SCID mice were purchased from Lasco Co., Ltd. (Taiwan) and were used for xenograft tumor models. Sh-YAP1 A549 cells were respectively transfected with 2 μ g vector control, 2 μ g YAP1 WT and 2 μ g YAP1 R331W plasmids for 48 hours and stable mix clones were selected by 400 μ g/ml of G418 and 2 μ g/ml of



puromycin for 7 days. The stably expressed cells of experimental groups (YAP1 WT and YAP1 R331W) were subcutaneously injected into 6 weeks NOD-SCID mice along with matrigel (right leg, 5×10^5 cells for YAP1 WT and YAP1 R331W group; left leg, 1×10^6 cells for vector control). Every 3-4 days, the tumor size was measured using calipers. The mice were sacrificed at 51 days, at which time the tumors were weighed and embedded in paraffin.

Immunoprecipitation

All experiments were performed in accordance with standard protocols as previously described (44). For co-immunoprecipitation, cell lysates were prepared with IP lysis buffer containing EDTA-free protease inhibitor (Roche). The 500ug protein lysates were incubated overnight at 4°C with 1 μ g of anti-Flag antibody (Santa Cruz Biotechnology, Dallas, Texas). The samples were incubated for 1h at 4°C with protein A/G Agarose beads (Santa Cruz Biotechnology), and the bound beads were washed with TBS buffer. The protein samples were separated by 8%~12% SDS-PAGE and analyzed by Western blot assay.



Nuclear and cytoplasmic extraction

The extracted nuclear and cytoplasmic protein fractions were conducted by using a nuclear/cytosol fractionation kit (BioVision, Mountain View, CA) following the manufacturer's protocol. Briefly, cells were collected and cytoplasmic extraction buffer A mixture (containing DTT and protease inhibitors) and CEB-B were added consecutively to extract the cytoplasmic proteins. Nuclear extraction buffer (NEB) mix (containing DTT and protease inhibitors) was added and the nuclear extract was separated by centrifugation.

Statistical analysis

The statistical tests without annotations were two-sided Student t test, and P-value < 0.05 was considered statistically significant. When appropriate, the results are presented as the means \pm SD. SPSS version 13.0 was used for above statistical analyses. The Kaplan-Meier method was used to estimate survival outcome and were compared using the log-rank test. The log-rank test was two-sided, and a P-value < 0.05 was considered statistically significant.

Results

Part-I



MiR-10a* expression associates with poor survival in lung adenocarcinoma

To find out the miRNAs, which are involved in the invasion process, the invasion abilities of 16 lung adenocarcinoma cells were measured by *in vitro* invasion assays, and clustered into high invasive group and low invasive group based on the comparison with CL1-0 cells which is originally derived from Taiwanese lung adenocarcinoma patients and defined as a low invasive cell line in our previous studies (Figure 1) (45, 46). The miRNA expression of 16 lung adenocarcinoma cells was profiled by the miRNAs expression arrays and subjected to log 2 transformation and quartile normalization. The miRNAs of high invasive cells with greater than 2-fold change compared with that of low invasive cells were selected under FDR protection ($p < 0.05$). Six out of 1146 miRNAs showed significantly associated with their invasion abilities (Figure 2A). Four miRNAs, miR-10a, miR-10a*, miR-335* and miR-149, were increased in high invasive cells and the other 2 miRNAs, miR-146b-5p and miR-598, were decreased (Table 2). To evaluate whether these miRNAs are associated with patients' outcome and play a role in



cancer progression? Six miRNAs expression of 98-lung adenocarcinoma patients were measured by qRT-PCR and correlated to patients' survivals. The clinicopathological characteristics of patients were listed (Table 3). The Kaplan-Meier analysis found that only the miR-10a* expression is associated with the poor overall and relapse-free survivals (Figure 3A and Figure 3B). Table 4 showed that the hazard ratio of miR-10a* for overall survival was 1.179 (95%CI: 1.005–2.798, $p=0.044$). Given that miR-10a* and miR-10a are derived from the same pre-miRNA and the abundance of miRNA-10a is much higher than miR-10a*, we calculated the expression levels of miRNA-10a* and miRNA-10a in 16 cell lines and 98 adenocarcinomas. The miR-10a expression is higher than miR-10a* up to 56-fold and 93-fold in cell lines and clinical specimens, respectively (4.48 \pm 4.97 vs. 0.08 \pm 0.10 in cell lines, 14.03 \pm 15.08 vs. 0.15 \pm 0.39 in adenocarcinomas). Moreover, we found that the miR-10a* expression is positively correlated to the invasive abilities in 16 lung adenocarcinoma cells ($r=0.6511$, Figure 4). These data implied that miR-10a* might have metastatic activity.

MiR-10a* promotes cell invasion *in vitro*

Given the limited studies of miR-10a* reported, we first carried out the transcriptional microarrays in miR-10a*-transfected and mock control HOP-62 cells and analyzed by

Metacore software (MetaCore, GeneGo Inc. St. Joseph, MI) to address why and how

miR-10a* associates with poor survival. The expressions of 1,716 genes and 2,145 genes

were significantly up-regulated or down-regulated with greater than 1.3-fold change in

miR-10a* transfected cells compared with mock control cells. The pathway analysis

revealed that five out of Top-10 ranking pathways are invasion/metastasis related (Table

4). This data implied that miR-10a* might accelerate cancer progression through

promoting cancer metastasis. To further address the role of miR-10a* in invasion, the

antagomir-10a* precursor was introduced into two high invasive cell lines, HOP-62 and

H1650. Knockdown of miR-10a* expression caused a significant decrease of

invasiveness in HOP-62 and H1650 cells (Figure 5). The results suggested that miR-10a*

might act as an oncogenic miRNA in lung adenocarcinoma.

HDAC5 is a miR-10a* target

To investigate the underlying mechanism of miR-10a*-inducing invasion, the potential

targets of miR-10a* were predicted by microcosm (<http://www.ebi.ac.uk/enright-srv/>

microcosm/cgi-bin/targets/v5/) miRNA-target prediction algorithms because most of the

popular miRNA target prediction algorithms do not include miR-10a*. Total of 793

potential miR-10a* targets were identified and HDAC5 was ranked number four. The



down-regulation of HDAC5 has been reported in several cancers including lung cancer (23, 25), however, the role of HDAC5 in cancer progression is controversial and largely unknown (26). Although HDAC5 is not the predicted target of miR-10a, it is still not to absolutely exclude the possibility HDAC5 suppression is caused by miR-10a through an unknown mechanism. To further confirm that HDAC5 is the target of miR-10a*, the miR-10a* precursor was transduced into two lung adenocarcinoma cell lines, HOP-62 and H1650 as well as two primary cultured cell lines from Taiwanese lung adenocarcinoma patients, CL-83 and CL-152. The protein levels of HDAC5 were measured by Western blot assays. We found that miR-10a*, but not the negative control precursor, was able to reduce the protein and RNA levels of endogenous HDAC5 (Figure 7A and Figure 7B). Moreover, the expression of HDAC5 was suppressed by miR-10a* in a dose-dependent manner (Figure 6). To further investigate how miR-10a* can regulate HDAC5 expression, the miR-10a* binding sites of HDAC5 were predicted by RNA22 (41). Two potential miR-10a* binding sites were identified (Figure 8A). The 1,623 base-paired fragment of full-length wild-type 3'UTR (Wt) was amplified from HOP-62 cells and cloned into the luciferase reporter vector, pMIR and the site-specific mutagenesis was performed to generate the single binding site or double binding sites



mutated constructs, (BS1 Mut, BS2 Mut and BS1+2 Mut, Figure 8A and Figure 8B). The reporter assays showed that miR-10a* significantly suppresses the luciferase activity in the construct of Wt HDAC5 3'UTR and the miR-10a*-mediated inhibition is almost abolished in the construct of BS2 Mut HDAC5 3'UTR (Figure 8B). The data indicated that the binding site 2 at nucleotide 1537 to 1558 is the major binding site responsible for miR-10a* suppression. To explore whether the regulatory relationship between miR-10a* and HDAC5 actually exist clinically the expressions of HDAC5 and miR-10a* were measured by immunohistochemistry staining (IHC) and qRT-PCR, respectively. Consistently, the expression of HDAC5 was negatively correlated with miR-10a* expression in 24 lung adenocarcinoma patients ($r=-0.404$, Figure 9A and 9B). Taken together, our data indicated that HDAC5 is a direct target of miR-10a* in lung adenocarcinoma.

HDAC5 attenuates the invasive ability of lung adenocarcinoma cells

Next, the impact of HDAC5 on invasiveness was explored by the transwell invasion assays and HDAC5 RNA silencing. First, two HDAC5 siRNAs were purchased from Ambion (Cat. No. s19462 and s19463) to evaluate the knockdown efficiency of endogenous HDAC5 in HOP-62 cells by qRT-PCR (Figure 10A). The data indicated that

the prior one, named as si-HDAC5, has stronger inhibitory activity on HDAC5 RNA expression. The HOP-62 and H1650 cells were transfected by HDAC5 siRNAs and assayed for invasion activity. We found that knockdown of endogenous HDAC5 expression enhances the invasive ability up to 2.70- and 2.19-fold compared with cells treated with si-NC in HOP-62 and H1650 cells, respectively (Figure 10B). To understand what proportion of miR-10a*-mediated invasion increase is HDAC5 dependent or not HOP-62 cells were introduced miR-10a* and ectopically expressed HDAC5 and analyzed by transwell invasion assays. First, the overexpression of miR-10a* enhanced the invasive ability of HOP-62 cells with 2.63-fold that is consistent with the findings obtained from miR-10a* silencing (Figure 5 and Figure 11). Importantly, we found that the overexpression of HDAC5 almost abolish the miR-10a*-induced invasiveness (Figure 11). To further confirm this findings we conducted an reverse experiment HOP-62 cells were transiently transfected with antago-miR-10a* precursor and HDAC5 siRNA and assayed for invasion activities. The results showed that miR-10a* knockdown attenuates the invasiveness to 47% compared with the anti-miR-NC mock control and the invasion suppression is totally abolished by HDAC5 siRNA (Figure 12). All these evidence demonstrated that miR-10a*-mediated invasive ability is mainly

through negative regulation of HDAC5 expression in lung adenocarcinoma cells.

Mechanism of miR-10a*-induced invasiveness

To explore the underlying mechanism of miR-10a*-regulated HDAC5 by which inhibits cell invasion, the transcriptomic analysis of HDAC5-expressing and mock HOP-62 cells were performed by microarrays and pathway analysis software (MetaCore, GeneGo Inc. St. Joseph, MI). Given that five out of Top-10 miR-10a*-altered pathways are invasion/metastasis related, the differentially expressed genes induced by HDAC5 involved in invasion process including adhesion and cytoskeleton remodeling were further investigated (Table 5). Among these pathways, only the ECM remodeling showed significantly associated with HDAC5 overexpression in which the MMP-2 expression was decreased. MMP2 is known an important metastasis promoting mediator in lung cancer together with MMP9 (47). To confirm and evaluate the suppressive activity of HDAC5 on metalloprotease expression, the mRNA expression and activity of the MMP-2 and MMP-9, were measured by qRT-PCR and Gelatin-zymography assays. Both expression and activity of MMP-2 and MMP-9 were reduced by HDAC5 (Figure 13). Next, to investigate how HDAC5 down-regulated the expression of MMP-2 and MMP-9, two transcription factor (TF) binding site prediction algorithms, PROMO and

JASPAR (48, 49), were applied to predict the TF binding sites on the regulatory regions

of MMP-2 and MMP-9 reported, respectively (Ref MMPs promoter). The union of

resulting TFs was intersected with the HDAC5-altered genes from microarray data of

HDAC5-expressing HOP-62 cells. Four TFs were identified in which the expression of

ATF3, GATA2 and NFkB is up-regulated and c-Fos is down-regulated (Table 6). The

role of ATF3, GATA2 and NFkB in the down-regulation of MMPs was not further

investigated because these TFs act as activator in transcriptional regulation, generally.

The down-regulated expression of c-Fos agreed with the down-regulated expression of

MMPs. Furthermore, AP1 was the only one common TF involved in MMP-2 and

MMP-9 regulations. To confirm whether MMP-2 and MMP-9 are transcriptionally

regulated by HDAC5-mediated AP1 the MMP-2 and MMP-9 promoter assays were

performed. First, we found that the mRNA expression of c-Fos and c-Jun were

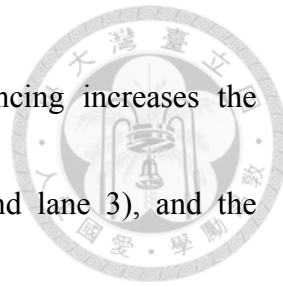
suppressed by HDAC5 assayed by qRT-PCR (Figure 14). To evaluate the impact of AP1

on MMP-2 and MMP-9 transcriptions the full-length regulatory fragments of MMP-2 (-1

to -1715) and MMP-9 (-1 to -1200) were cloned into the pGL4.17 reporter vector (50,

51). First we found that silencing of c-Fos inhibits the basal promoter activities of both

MMPs (Figure 15, lane 1 and lane 2). It implied that AP1 is indeed involved in MMP

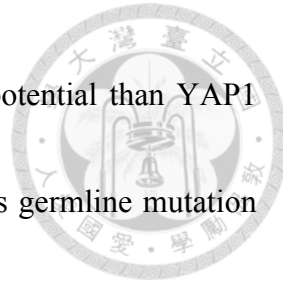


expression. The luciferase assay then showed that HDAC5 silencing increases the promoter activities of MMP-2 and MMP-9 (Figure 15, lane 1 and lane 3), and the up-regulated activities of MMP-2 and MMP-9 are totally abolished by c-Fos silencing (Figure 15, lane 3 and lane 4). Finally, the impact of MMPs on the miR-10a*-mediated increasing invasiveness was further investigated. First, the qRT-PCR assays found the overexpression of miR-10a* enhanced the MMP-2 and MMP-9 mRNA expression (Figure 16) and the invasion assays showed overexpression of miR-10a* increases the invasive capability of HOP-62 cells but the induction is abolished by either MMP-2 silencing or MMP-9 silencing (Figure 17). Taken together, the increase of invasiveness induced by miR-10a* is mainly through upregulation of MMP-2 and MMP-9. Figure 18 summarizes the signaling pathway of miR-10a*-mediated invasive increase in which miR-10a* up-regulates AP1 activity through targeting HDAC5. The increased AP1 augments MMP-2 and MMP-9 activity resulting invasion induction.

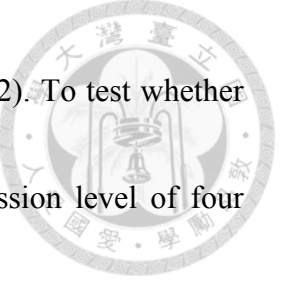
Part-II

YAP1 R331W mutation increased colony formation *in vitro* and *in vivo*

According to our prior research, we have identified YAP1 germline mutation R331W



possessed the much stronger colony-forming ability and invasion potential than YAP1 WT in lung adenocarcinoma cells (38). First, to answer whether this germline mutation could play the driving role in the development of lung cancer, plasmids (vector, YAP1 WT and YAP1 R331W) were respectively transfected into normal human lung cells BEAS-2B. The result of anchorage-independent colony formation assay showed that there is no significant difference either for vector group and WT group, or between WT group and YAP1 R331W group (Figure 20). Next, to investigate why and how R331W mutation triggers much more malignant phenotypes than YAP1 WT group, plasmids (vector, YAP1 WT and YAP1 R331W) were respectively transfected into A549 cells stably expressing sh-YAP1. Interestingly, we found that both the number of colonies and the average size of each colony in YAP1 R331W treatment were significantly formed much larger than YAP1 WT treatment (Figure 21). Furthermore, the stably expressed A549 cells (Two paired groups, vector and YAP1 WT, vector and YAP1 R331W) were subcutaneously injected in different legs of 6 weeks NOD-SCID mice. To clearly determine the difference on tumorigenesis between YAP1 WT and YAP1 R331W, the number of vector control was 2-fold greater than other two groups. The results showed that both the average tumor weight and the tumor volume of YAP1 R331W group were



significantly increased much greater than YAP1 WT group (Figure 22). To test whether YAP1 R331W mutation play a role in stemness, the relative expression level of four markers were determined by using qRT-PCR. We found that only the relative expression level of Oct4 and Sox2 can be up-regulated by YAP1 R331W much higher than YAP1 WT group (Figure 23).

YAP1 R331W mutation promoted invasiveness *in vitro*

TAZ, a YAP paralog gene in vertebrates and also was isolated as 14-3-3 binding protein (52). Moreover, YAP/TAZ are major determinants of malignancy in several human cancer. Herein, we supposed that TAZ expression might compete with YAP1 on influence of malignant phenotypes. To clearly determine the effect of YAP1 on malignancy in lung adenocarcinoma, sh-YAP1 A549 cells were infected with sh-TAZ lentivirus. Interestingly, we found that the invasiveness of YAP1 R331W was significantly increased much higher than YAP1-WT group (Figure 24). Besides, relative expression level of MMP9 was enhanced by YAP1 R331W overexpression much higher than YAP1-WT group (Figure 24).

The potential YAP1 R331W mediated-mechanisms in lung adenocarcinoma



To investigate why and how YAP1 R331W mutation contributes much more malignant effect than YAP1 WT in lung adenocarcinoma cells, the mechanisms of both genotypes were compared and analyzed. We showed that ectopic YAP1 R331W mutation expression obviously increased much higher nuclear accumulation of YAP1 than ectopic YAP1 WT expression in A549 YAP1 knockdown cells (Figure 25). Besides, ectopic YAP1 R331W mutation significantly decreased much lower phosphorylation of cytoplasmic YAP1 Ser127 expression in YAP1 knockdown A549 cells (Figure 25).

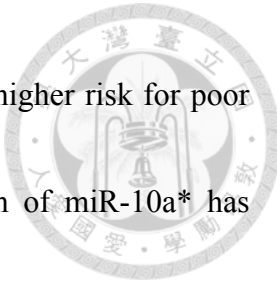
Discussion

Part-I



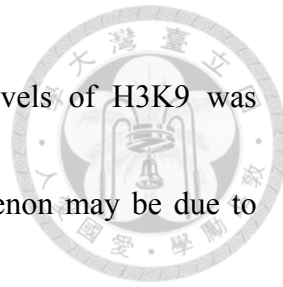
Previously we correlated the gene expressions of lung cancer cell lines with cell invasive capabilities and identified a prognostic four-gene signature for predicting the survival of lung cancers (40). Taking the advantage of this study, we extended the analysis from lung cancer lines to all of NCI-60 cell lines and identified an other invasion-related eight-gene signature by which the chemosensitivity of cell lines and the relapse-free survival of lung cancers and breast cancers can be predicted, recently (53). Although the miRNAs have been approved in the development of miRNAs-based diagnostic and prognostic biomarkers as well as anticancer therapeutic agents (39) the role of miRNAs and the underlying mechanism involved in invasion metastasis of lung cancer is not fully understood.

In this study, we started from the genomewide miRNAs profiling of 16 lung adenocarcinoma cells and correlated the miRNA expressions to the invasive capabilities of these cell lines. Six invasion-associated miRNA candidates were identified and evaluated for the prognostic prediction by a clinical cohort of 98 lung adenocarcinoma patients. We found that only the miR-10a* expression is significantly associated with the



shortened outcome. Patients with high miR-10a* expression have a higher risk for poor overall and relapse-free survivals. The role and biological function of miR-10a* has never been reported in lung cancer before, up to our best knowledge. Until now, only three papers studied the functions of miRNA-10a*, up to our best knowledge. Dr. Ujifuku et al. have identified that miR-195, miR-455-3p and miR-10a* may play roles in acquired temozolomide (TMZ) resistance of glioblastoma multiforme (GBM) (54). Another study showed that miR-10a* and miR-21 regulate endothelial progenitor cells (EPC) senescence via suppressing Hmga2 expression (55). MiR-10a* has been found to positively modulate the biogenesis of Group B coxackievirus (CVB3) and to involve in cardiac pathogenesis (56). In this study, we proved that HDAC5 acts as a target of miR-10a* and is responsible for the miR-10a*-mediated phenotypic alterations in lung adenocarcinoma.

Lysine acetylation, one kind of histone modification, is an important epigenetic regulation involved in tumorigenesis and metastasis (57). Hyper-acetylation of histone 3 at lysine 9 (H3K9ac) was significantly associated with the poor survival of stage I lung adenocarcinoma (58). In the liver as well, higher acetylation of histone H3K9 was detected in hepatocellular carcinoma than in normal or cirrhotic precursor lesions (59).



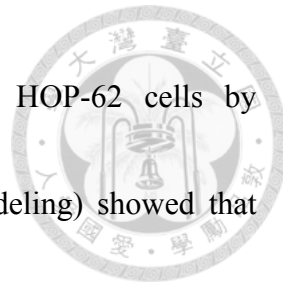
Conversely in the prostate adenocarcinoma, higher acetylation levels of H3K9 was associated with better prognosis (60). Such heterogeneous phenomenon may be due to different mechanisms and specificity of acetylation sites in different cancer types. The acetylation status of histones was dynamically regulated by histone lysine acetyltransferases (HATs) and HDACs and determined the transcription of genes (61). Currently, HDAC inhibitors (HDACi) were widely evaluated and treated as anticancer drugs due to upregulation of HDACs in cancers and low toxicity to patients. Some HDACi (Vorinostat, Romidepsin, Belinostat, Panobinostat) have been granted FDA approval for cancer and several HDACis are currently in different phases of clinical trials (62). On the other hand, the controversial findings were reported. HDACi can trigger apoptosis process by upregulating p21 (63) but enhances metastasis through upregulation of uPA in neuroblastoma and prostate cancer cells (64). Dr. Jou reported that HDACi augmented cell migration and metastasis through induction of PKCs and MMPs expression (65). However, the role of class II HDACs in cancer progression remains largely unknown, particularly HDAC5 even though the reduced expression of HDAC5 has been reported to be associated with the unfavorable outcome in a related small cohort of NSCLC patients (23). To further characterize the regulation and biological functions



of HDAC5 is critical for the development of HDAC-based regiments. Herein, we were first time to demonstrate the inhibitory function of HDAC5 on the invasiveness in lung adenocarcinoma, up to our best knowledge. Most importantly, we clearly demonstrated that HDAC5 inhibits the expression of c-Fos and c-Jun by which a lot of AP1-regulated genes are down-regulated. Previous studies have reported that AP-1 activation can enhance the expression of MMP-2 and MMP-9 (66, 67). Our data might partly explain the conflict findings of HDACs in the insufficient efficacy of HDACi and the influence on cancer progression *in vitro* and *in vivo*.

MMPs, zinc-dependent endopeptidases, can degrade the extracellular matrix. They play many important roles such as cell migration, adhesion, cell proliferation, angiogenesis and apoptosis. MMP-2 and MMP-9, are two widely studied MMPs, can regulate cell migration and invasion (68-70). Our data indicated that HDAC5 could suppress the gene expression and activity of MMP-2 and MMP-9. Because Dr. Song found that HDAC10 may be recruited to MMP9 promoter region by interacting with transcription factor p65 (68). We can not exclude the possibility whether HDAC5 suppresses MMP expression via HDAC5 and AP1 interaction at protein level.

In addition to miR-10a*/HDAC5/AP1 axis, the altered expression of several



invasion-related genes were found in the miR-10a*-expression HOP-62 cells by microarray analysis. The first ranked pathway (cytoskeleton remodeling) showed that Urokinase plasminogen activator (uPA), p38 and MEK were increased, however, PAI-1 was decreased (Supplementary Table 3 and Supplementary Figure 3C). uPA may mediate tumor invasiveness through the conversion of plasminogen to plasmin, which can degrade basal membrane (71). Plasminogen activator inhibitor-1 (PAI-1) also known as SERPINE1, a serine protease inhibitor, also is the principal inhibitor of tissue plasminogen activator (tPA) and uPA. Plasmin is considered as the most significant activator of pro-MMPs in extracellular space. Previous study has indicated the important of p38 MAPK in invasion and metastasis (72). Besides, another study reported that the inhibition of the p38 MAPK leads to decreased phorbol ester-induced MMP-9 expression and invasion by tumor cells (73).

Part-II

In our result of part I, the array of miR-10a*/NC Chen discovered that YAP1 R331W as an allele predisposed for lung adenocarcinoma with high familial penetrance (38). Though the growing evidence elucidates the role of YAP as a major controller of organ size and as a human oncogene, the biological information and the underlying mechanism

of YAP1 R331W remains unknown. In this study, we firstly found that YAP1 R331W germline mutation significantly promoted tumor growth *in vitro* and *in vivo*. The Hippo pathway is the only inhibitor of YAP1. Zhao et al. had elucidated a clear model of YAP inhibition by Hippo pathway and CK1. When Hippo pathway is activated, both the S127 and S381 sites of YAP will be phosphorylated in the HXRXXS motifs. Phosphorylation of S127 leads to both of the 14-3-3 binding and cytoplasmic retention of YAP. Therefore, YAP can be inhibited by separation from its nuclear target transcription factors, such as TEADs. This mechanism of regulation is reversible. In our study, we observed that ectopic YAP1 R331 expression increases nuclear accumulation and decreases phosphorylation of YAP1 S127 in YAP1 knockdown lung adenocarcinoma cells. YAP1 is found in the cytoplasm and in the nucleus, where it regulates gene transcription, YAP1 nuclear accumulation is a key determinant of its function. Phosphorylation of YAP1 S127 creates a binding consensus for 14-3-3 proteins, which could make YAP1 to stay in the cytoplasm (74). On the other hand, if YAP1 S381 site is phosphorylated by CK1 δ/ϵ , resulting in activation of a phosphodegron, and then recruits the SCF β -TRCP E3 ubiquitin ligase, leading to YAP degradation. This mechanism of regulation is irreversible (75). Our data show that YAP1 R331W can increase YAP1

protein stability at a higher degree than YAP1 WT group. Besides, proteasome inhibitor attenuates the YAP1 degradation in both of ectopically expressed YAP1 WT and YAP1 R331W groups. These suggested that YAP1 not only increases the YAP1 protein stability, but also protects YAP1 from proteasomal degradation. Moreover, ectopic YAP1 R331W expression increased much stronger YAP1-TEAD4 interaction than YAP1 WT group in lung adenocarcinoma cells. YAP1 function may underlie some of the hallmarks of cancer, such as uncontrolled proliferation, escape of cell death, and induction of cancer stem cells (76). We only found that YAP1 R331W can enhance the relative expression level of stemness markers Oct4 and Sox2 in lung adenocarcinoma cells. The role of YAP1 R331W in EGFR-target therapeutic drugs sensitivity is going to be investigated.



Figure 1

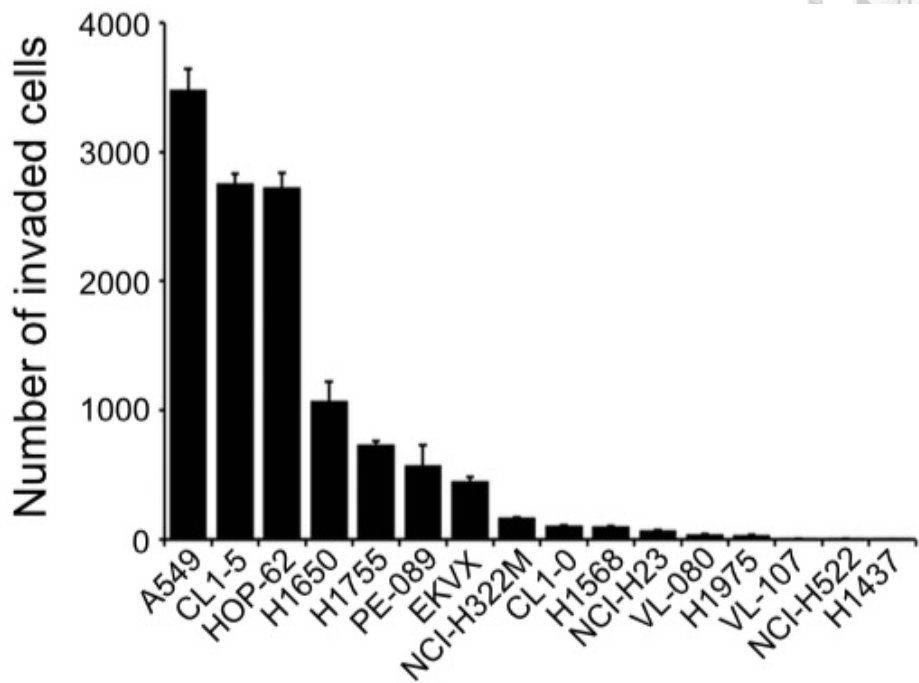


Figure 1 Invasion activity profile of 16 lung adenocarcinoma cells.

Invasiveness of sixteen lung adenocarcinoma cells showed different expression between two groups: highly invasive group (n=8; A549, CL1-5, HOP62, H1650, H1755, PE-089, EKVX and NCI-H322M) and lowly invasive group (n=8; CL1-0, H1568, NCI-H23, VL-080, VL-107, NCI-H522 and H1437). 1x10⁵ cells of each cell line were performed matrigel invasion assays.



Figure 2

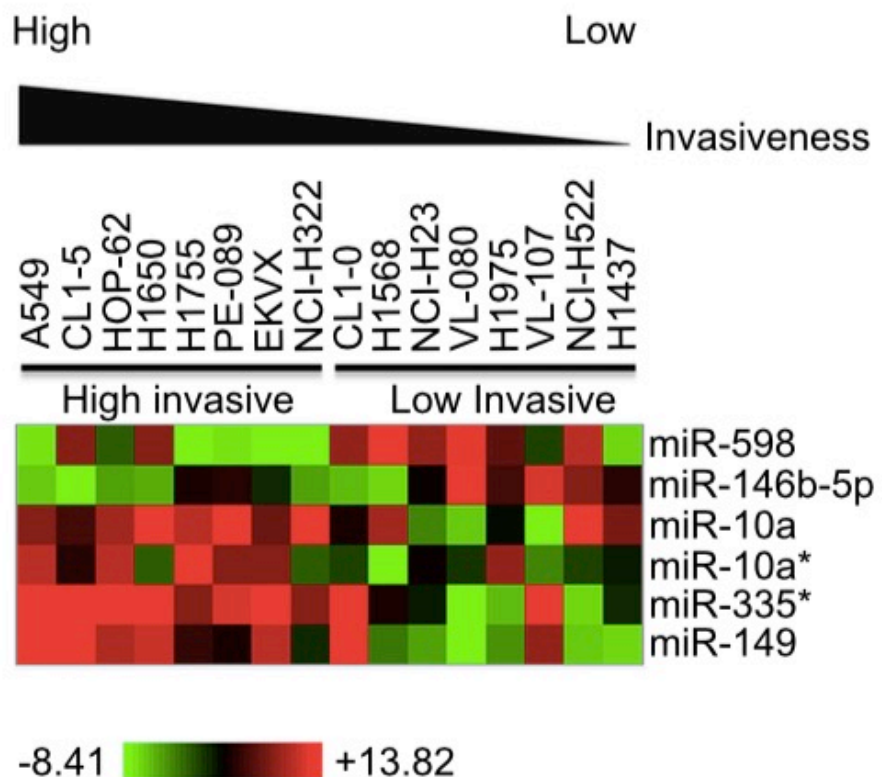


Figure 2 Each of six microRNAs expression was significantly correlated to invasiveness in lung adenocarcinoma cells.

microRNAs expression profiling of 16 lung adenocarcinoma cell lines were performed and compared with their invasiveness (high- and low-invasive group). Heat map presents the six microRNAs expression profiles of 16 lung adenocarcinoma cells.



Figure 3

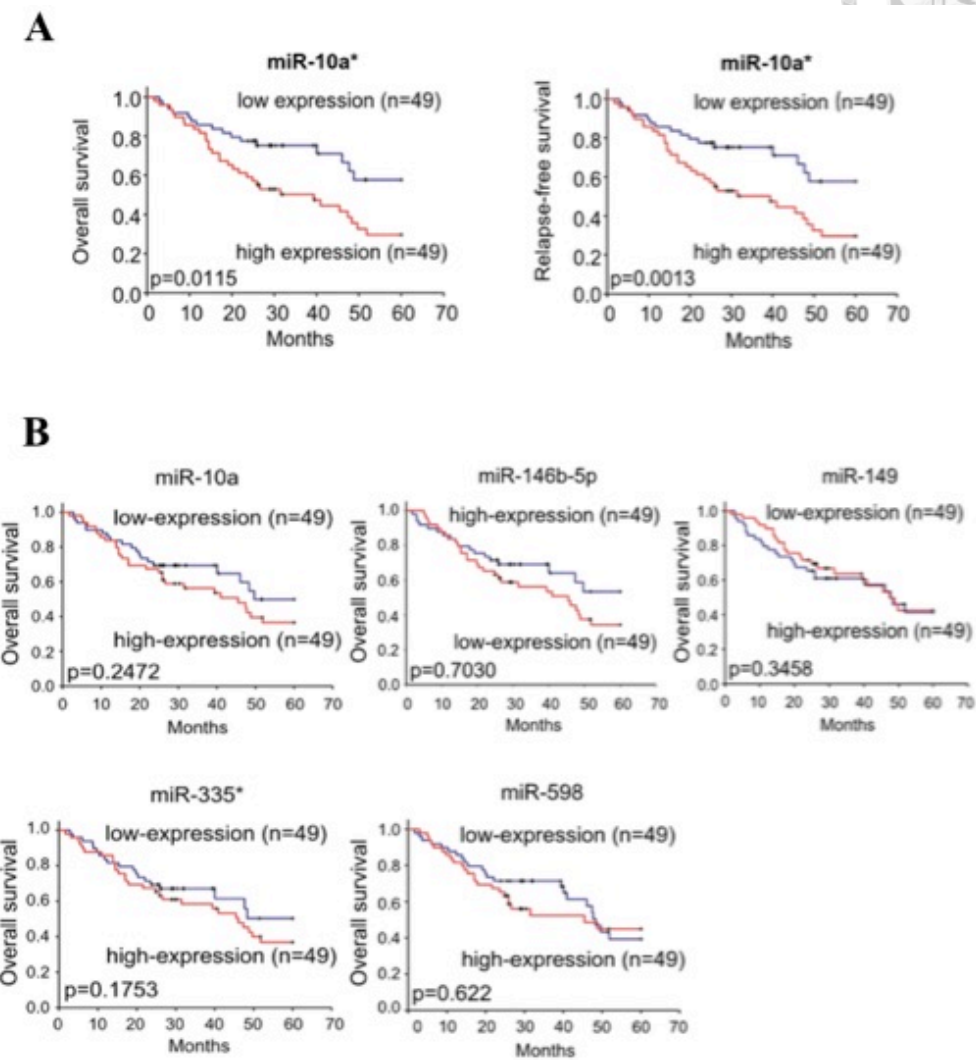


Figure 3 Patients with high miR-10a* expression were significantly correlated to poor outcome of Overall survival and Relapse survival.

A, Overall survival and Relapse survival were considered to relative miR-10a* expression.

B, The expression of other 5 miRNAs respectively shows no significantly correlation with Overall survival outcome of 98 lung adenocarcinoma patients.



Figure 4

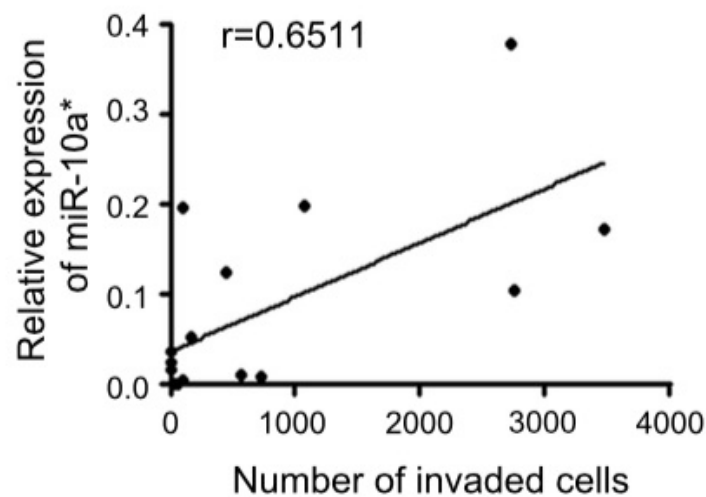


Figure 4 The expression of miR-10a* showed a moderate correlation with invasiveness of 16 lung adenocarcinoma cells.

Relative miR-10a* expression and invaded cell number are considered to the Regression and correlation analysis.

Figure 5

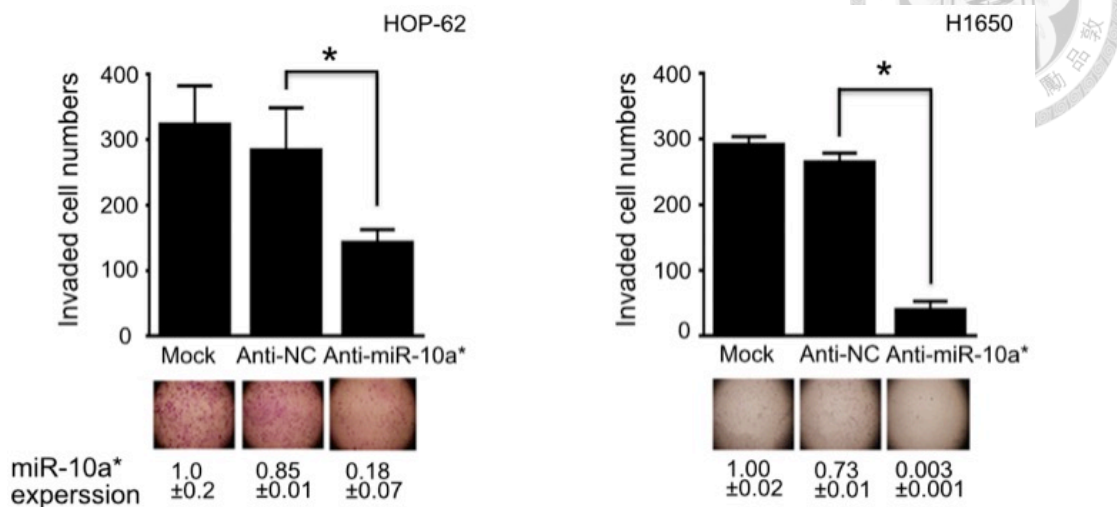


Figure 5 Inhibition of miR-10a* attenuated the invasion abilities of lung adenocarcinoma cell lines.

HOP-62 and H1650 were transfected with Anti-miR-10a* mimics for 48 hours and performed invasion assay. The relative miR-10a* expression was analyzed by RT-qPCR.

Means \pm SD., n=3; *P < 0.05 (two-tailed Student's t test).



Figure 6

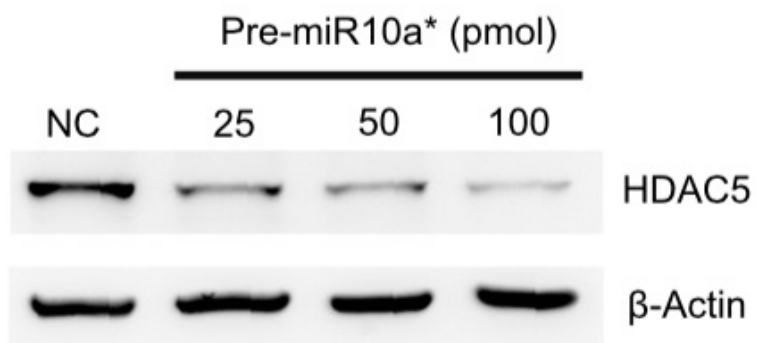


Figure 6 MiR-10a* decreased endogenous protein level of HDAC5.

HOP-62 cells were respectively transfected with Pre-NC and miR-10a* mimics for 48 hours and the HDAC5 protein expression was detected by Western blot assay with HDAC5 antibody. β-Actin served as an internal control.



Figure 7

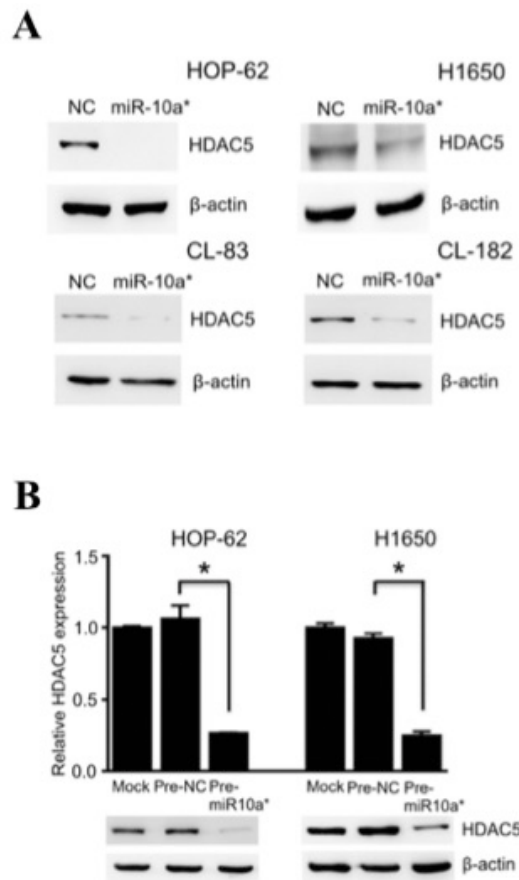


Figure 7 MiR-10a* significantly inhibited the protein and RNA levels of endogenous HDAC5 in lung adenocarcinoma cells.

A, Lung adenocarcinoma cells (CL-83 and CL-182 were established by Taiwanese lung cancer patients) were transfected with 100pmol miR-10a* mimics for 48 hours and the HDAC5 protein expression was detected by western blot assays. B, The relative HDAC5 mRNA expression was analyzed by RT-qPCR. Means \pm SD., n=3; *P < 0.05 (two-tailed Student's t test).



Figure 8

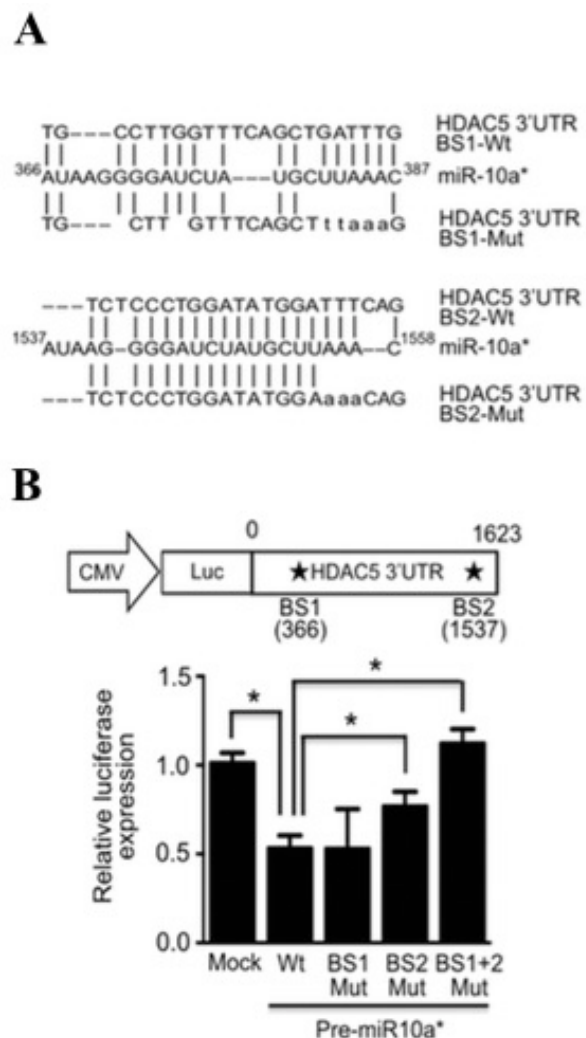


Figure 8 MiR-10a* significantly suppressed the luciferase activity in the

construct of wild-type HDAC5 3'UTR.

A, The predicted sequence of the miR-10a* binding sites within the Wt HDAC5 3'UTR.

The mutated binding sites sequences of ectopic constructions were also indicated. B,

HEK293T cells were respectively co-transfected with the reporter vector (pSilencer

vector, HDAC5 3'UTR-BS WT, BS1 Mut, BS2 Mut and BS1+2 Mut) and different dose

of miR-10a* mimics, as indicated, and firefly luciferase activity measured 48 hours later.

Means \pm SD., n=3; *P < 0.05 (two-tailed Student's t test).





Figure 9

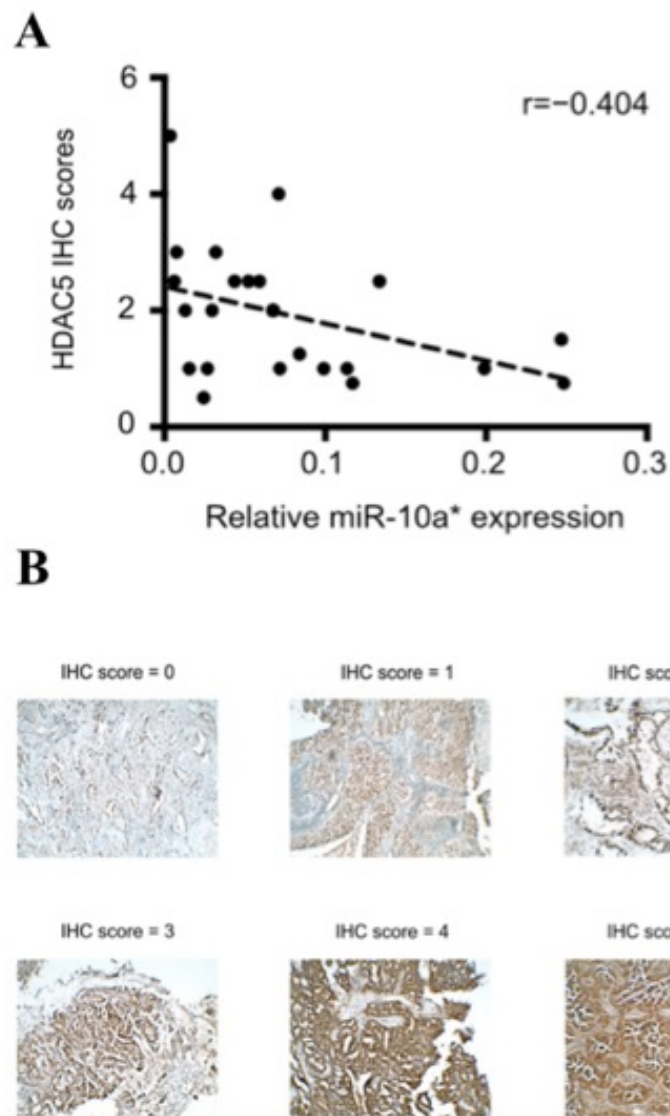


Figure 9 The expression of HDAC5 was negatively correlated with miR-10a* expression in lung adenocarcinoma patients.

A, IHC staining result of HDAC5 showed a moderate negative correlation with miR-10a* expression in 24 lung adenocarcinoma clinical samples. B, Each image of distinct IHC score was represented.



Figure 10

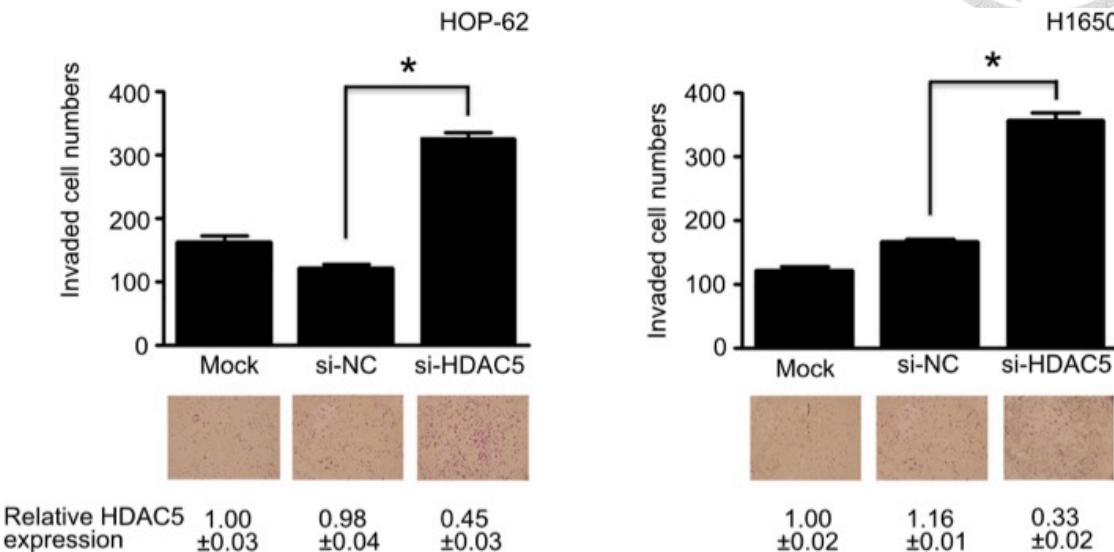


Figure 10 Inhibition of HDAC5 enhanced the invasiveness of lung adenocarcinoma cells.

A, HOP-62 cells were respectively transfected with control siRNA and 2 HDAC5 siRNAs for 48 hours and the relative HDAC5 expression was analyzed by qRT-PCR. B, HOP-62 and H1650 cells were transfected with si-HDAC5 mimics for 48 hours and performed the invasion assays. The relative HDAC5 mRNA expression was analyzed by qRT-PCR. In Error bars, means \pm SD., n=3; *P < 0.05 (two-tailed Student's t test).



Figure 11

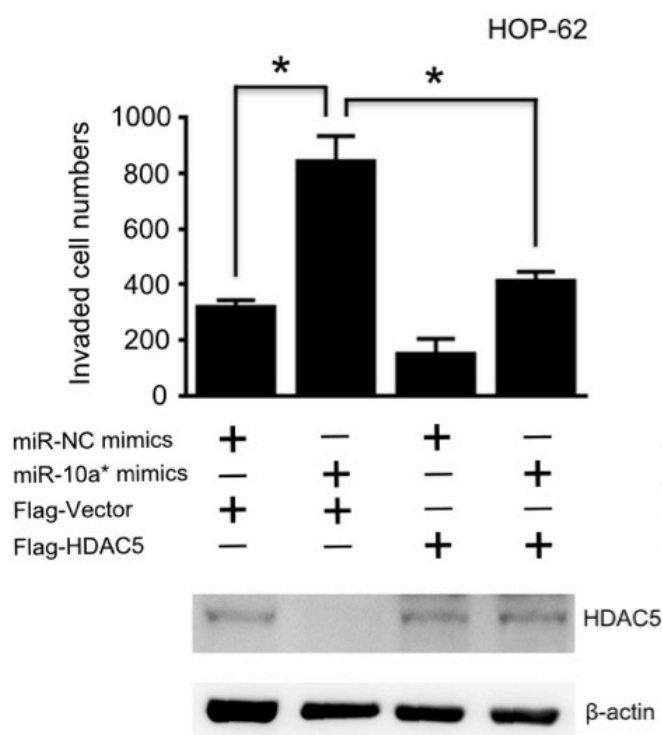


Figure 11 MiR-10a*-mediated invasive ability was attenuated by HDAC5 overexpression in lung adenocarcinoma cells.

HOP-62 cells were respectively co-transfected with miR-10a* mimics and Flag-HDAC5 CDS vector for 48 hours and performed the matrigel invasion assays. The HDAC5 and β-actin protein expression were analyzed by Western blot assays. *P < 0.05 (two-tailed Student's t test). The HDAC5 protein expression was detected by Western blot assays with HDAC5 antibody. β-actin served as an internal control.



Figure 12

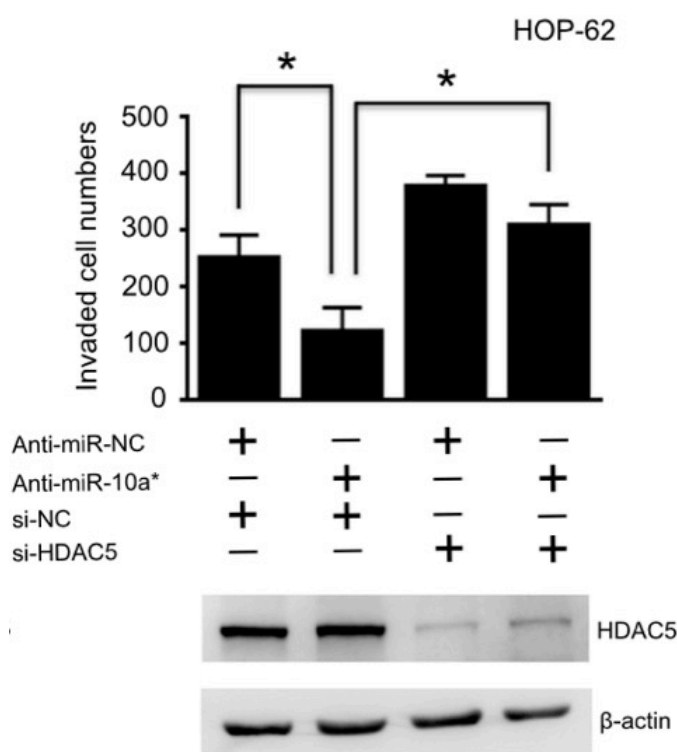


Figure 12 AntagomiR-10a*-decreased invasive ability was rescued by si-HDAC5

delivery in lung adenocarcinoma cell line HOP-62.

HOP-62 cells were respectively co-transfected with anti-miR-10a* mimics and HDAC5

siRNA for 48 hours and performed the matrigel invasion assays. The HDAC5 and

β-actin protein expression were analyzed by Western blot assays. *P < 0.05 (two-tailed

Student's t test).



Figure 13

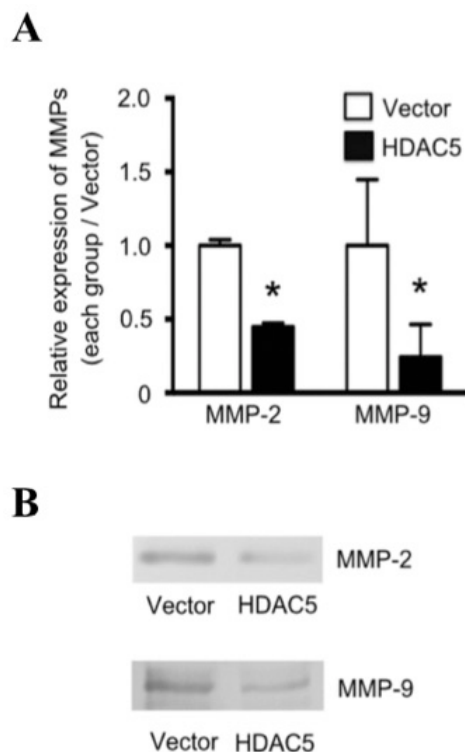


Figure 13 Overexpression of HDAC5 inhibited mRNA level and activity of MMP-2 and MMP-9.

A, HOP-62 cells were respectively transfected with Vector and Flag-HDAC5 for 48 hours and the relative MMP-2 and MMP-9 expression were analyzed by qRT-PCR. Means \pm SD., n=3; *P < 0.05 (two-tailed Student's t test, comparison of HDAC5 group versus vector group). B, overexpression of HDAC5 inhibits activities of MMP-2 and MMP-9. HOP-62 cells were respectively transfected with Vector and Flag-HDAC5 for 48 hours and the activities of MMP-2 and MMP-9 were performed by zymography assay.

Figure 14

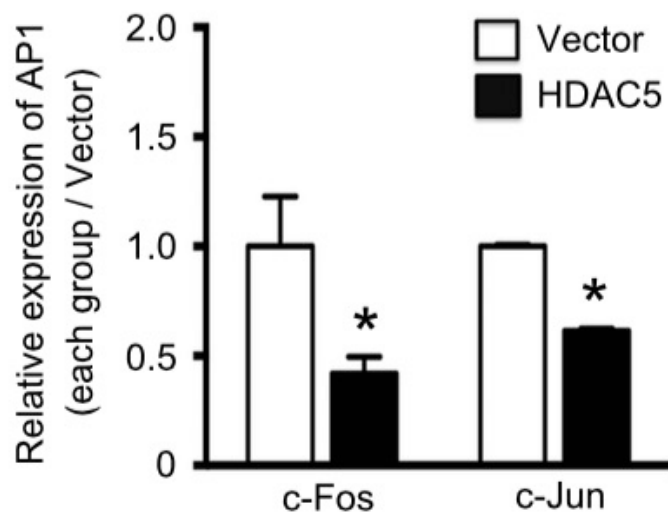


Figure 14 Overexpression of HDAC5 inhibited mRNA level of c-Fos and c-Jun.

HOP-62 cells were respectively transfected with Vector and Flag-HDAC5 for 48 hours

and the relative c-Fos and c-Jun expression were analyzed by qRT-PCR. Means \pm SD.,

n=3; *P < 0.05 (two-tailed Student's t test, comparison of HDAC5 group versus vector

group).

Figure 15

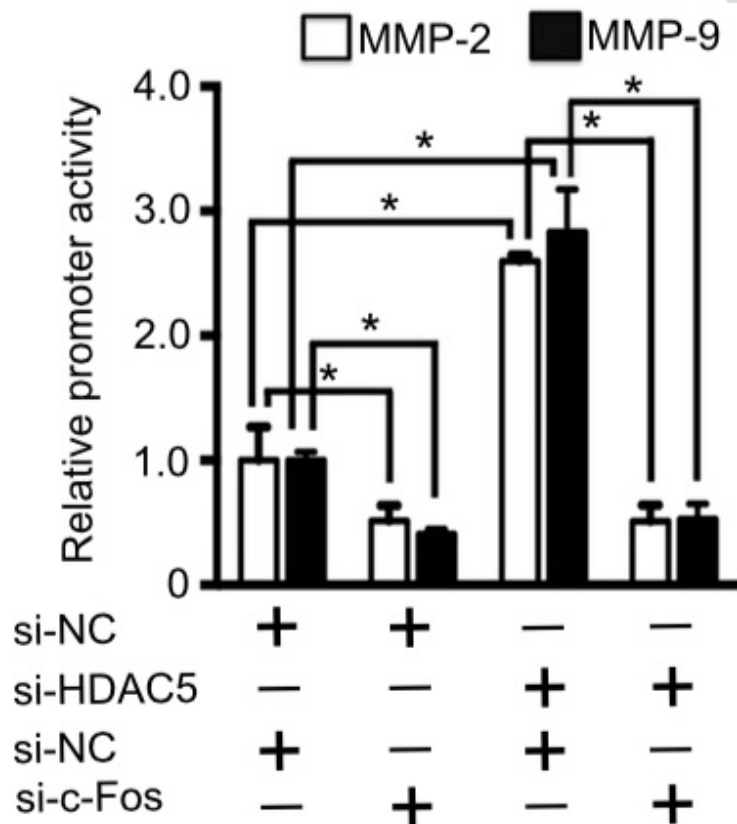


Figure 15 Lacking of c-FOS abolished si-HDAC5-enhanced MMP-2 and MMP-9

promoter activities.

HOP-62 cells were respectively co-transfected with si-HDAC5 mimics, si-c-FOS mimics

and luciferase reporter vector for 48h. Luciferase activity of each assayed condition

group was measured by luminescence reader and normalized to land 1 group. Renilla

luciferase was used as an internal control.



Figure 16

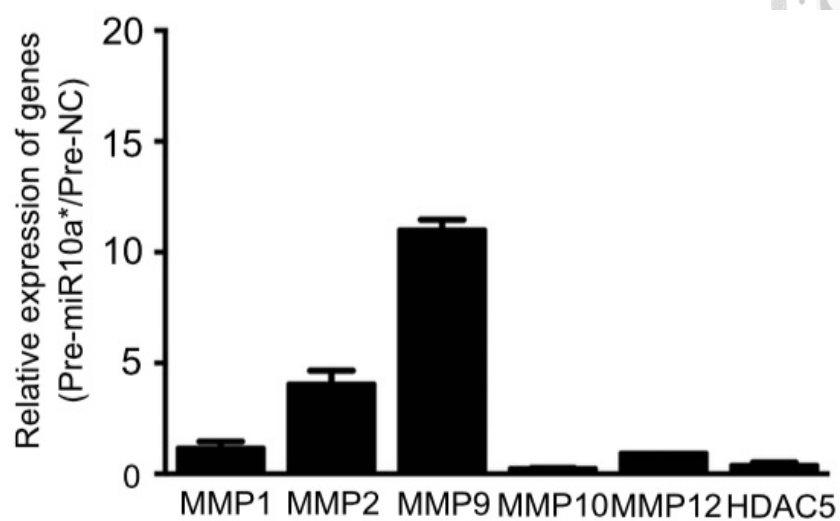


Figure 16 MiR-10a* enhanced MMP-2 and MMP-9 mRNA expression in lung

adenocarcinoma cells.

HOP-62 cells were transfected with negative control mimics and 100 pmol miR-10a* mimics for 48 hours and relative MMPs and HDAC5 expression were analyzed by qRT-PCR. Each ratio of Pre-miR-10a* to Pre-NC was represented.

Figure 17

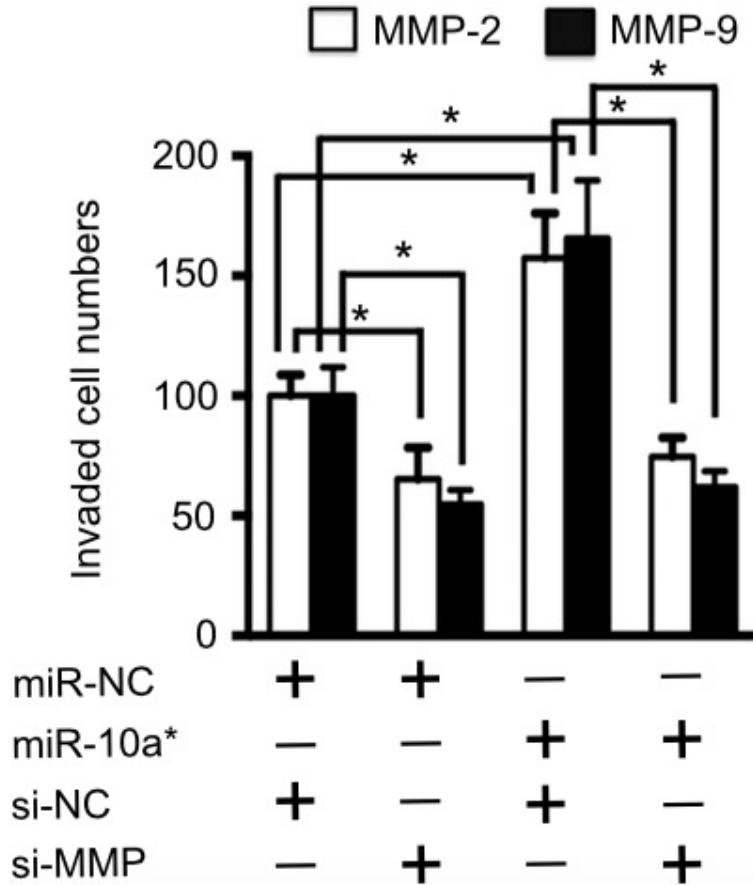


Figure 17 MiR-10a*-induced invasive ability was attenuated by si-MMP-2 and si-MMP-9 delivery in lung adenocarcinoma cell line HOP-62.

HOP-62 cells were respectively co-transfected with miR-10a* mimics and si-MMP-2 and si-MMP-9 mimics for 48 hours and performed the matrigel invasion assays. MMP-2 and MMP-9 mRNA expression were analyzed by RT-qPCR. *P < 0.05 (two-tailed Student's t test).



Figure 18

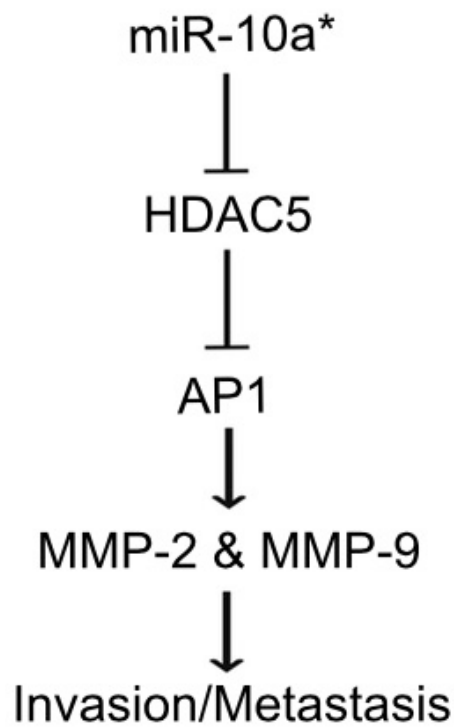


Figure 18 Model of miR-10a*-regulating network.

MiR-10a* promoted invasiveness by down-regulation of HDAC5/AP1 axis. All assays were performed in experiment.



Figure 19

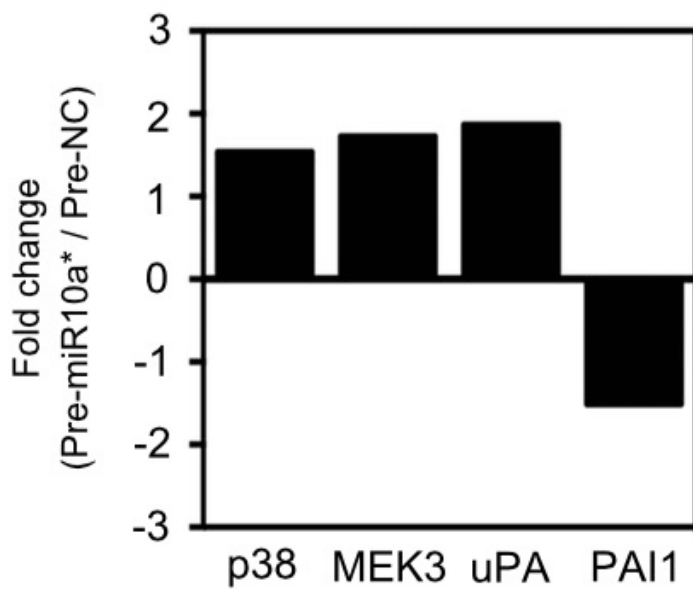


Figure 19 Microarray result indicated that transfection of miR-10a* can increase the relative fold change of p38, MEK3 and uPA.

HOP-62 cells were transfected with Pre-miR-10a* mimics for 48 hours and its RNA were performed with microarray assays. Each ratio of Pre-miR-10a* to Pre-NC was represented.



Figure 20

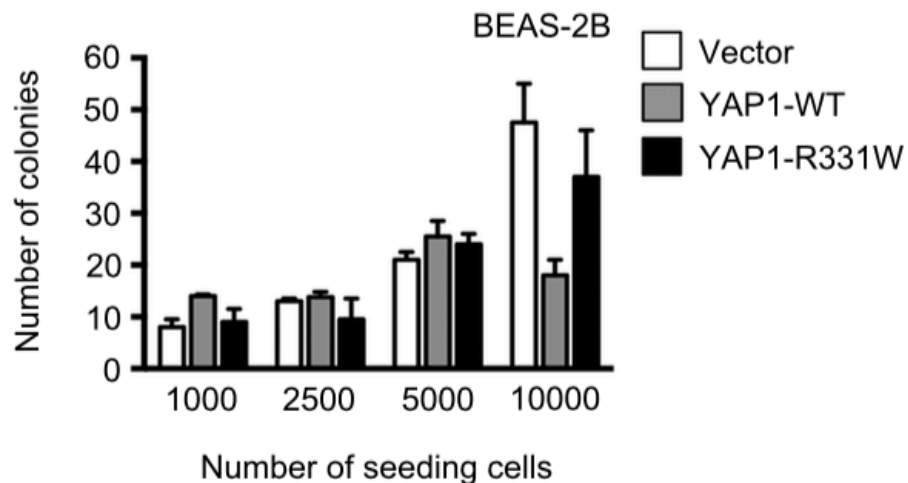


Figure 20 Overexpression of YAP1 R331W mutation did not play the driving role

in the development of tumorigenesis.

BEAS-2B cells were respectively transfected with 2 μ g Vector control , 2 μ g YAP1 WT and 2 μ g YAP1 R331W plasmids for 48 hours and stable mix clones were selected by 400 μ g/ml of G418 for 7 days. Anchorage-independent growth assay (soft agar assay) was sequentially conducted for 4 weeks. The number of colonies was counted under the microscope.

Figure 21

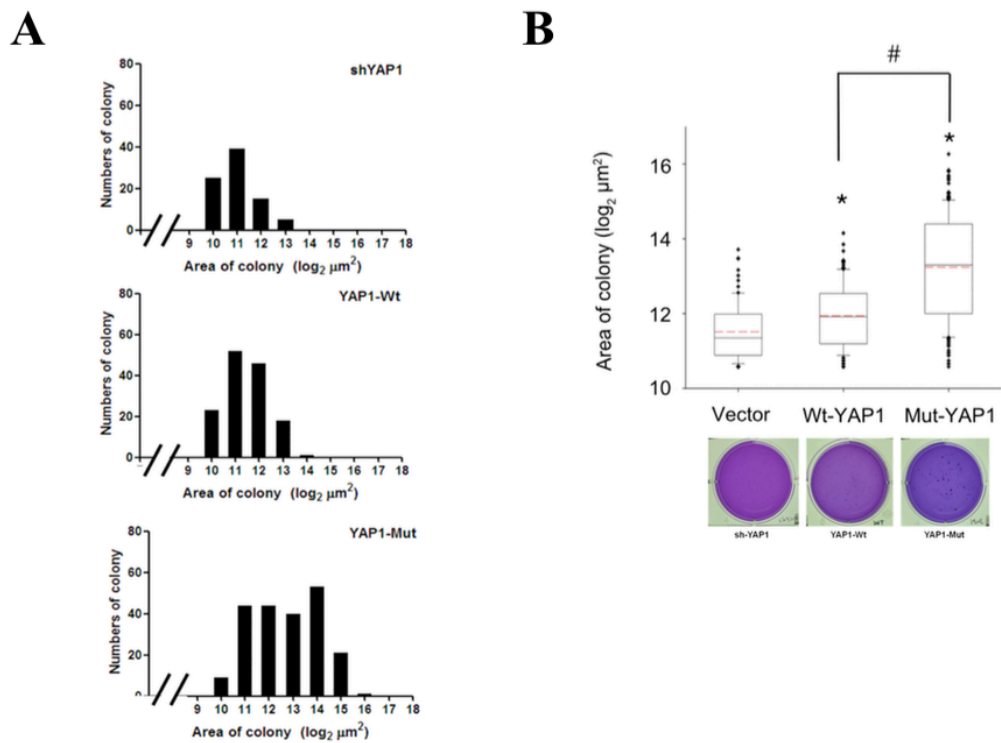


Figure 21 YAP1 R331W significantly increased the number of colonies and each area of colony *in vitro*.

YAP1 knockdown A549 cells were respectively transfected with 2 μg Vector control ,

2 μg YAP1 WT and 2 μg YAP1 R331W plasmids for 48 hours and stable mix clones

were selected by 400 $\mu\text{g}/\text{ml}$ of G418 and 2 $\mu\text{g}/\text{ml}$ of puromycin for 7 days.

Anchorage-independent growth assay (soft agar assay) was sequentially conducted for 4

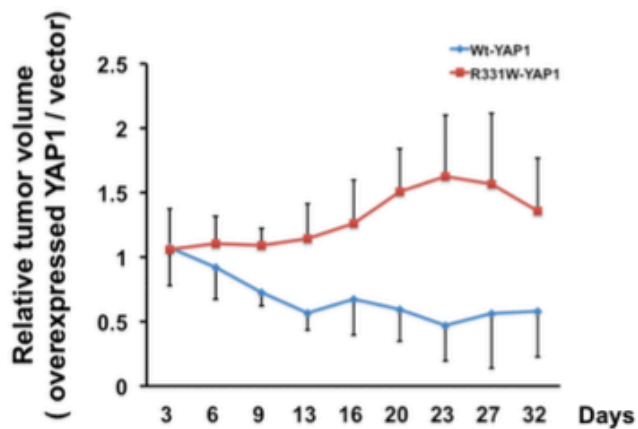
weeks. The number of colonies was counted under the microscope. The area of colony

was determined by using high content screening instruments.



Figure 22

A



B

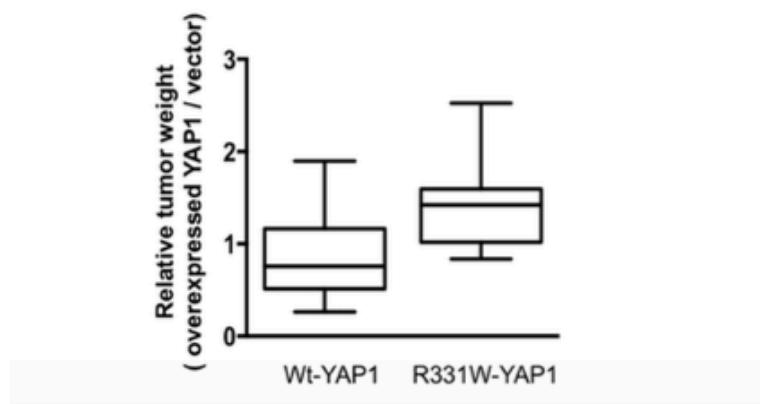


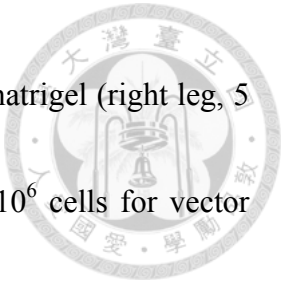
Figure 22 YAP1 R331W mutation increased colony formation *in vivo*.

YAP1 knockdown A549 cells were respectively transfected with 2 μ g vector control,

2 μ g YAP1 WT and 2 μ g YAP1 R331W plasmids for 48 hours and stable mix clones

were selected by 400 μ g/ml of G418 and 2 μ g/ml of puromycin for 7 days. The stably

expressed cells of experimental groups (YAP1 WT and YAP1 R331W) were



subcutaneously injected into 6 weeks NOD-SCID mice along with matrigel (right leg, 5 $\times 10^5$ cells for YAP1 WT and YAP1 R331W group; left leg, 1 $\times 10^6$ cells for vector control). A, every 3-4 days, the tumor size was measured using calipers. B, The tumors were weighed, at which time the mice were sacrificed.

Figure 23

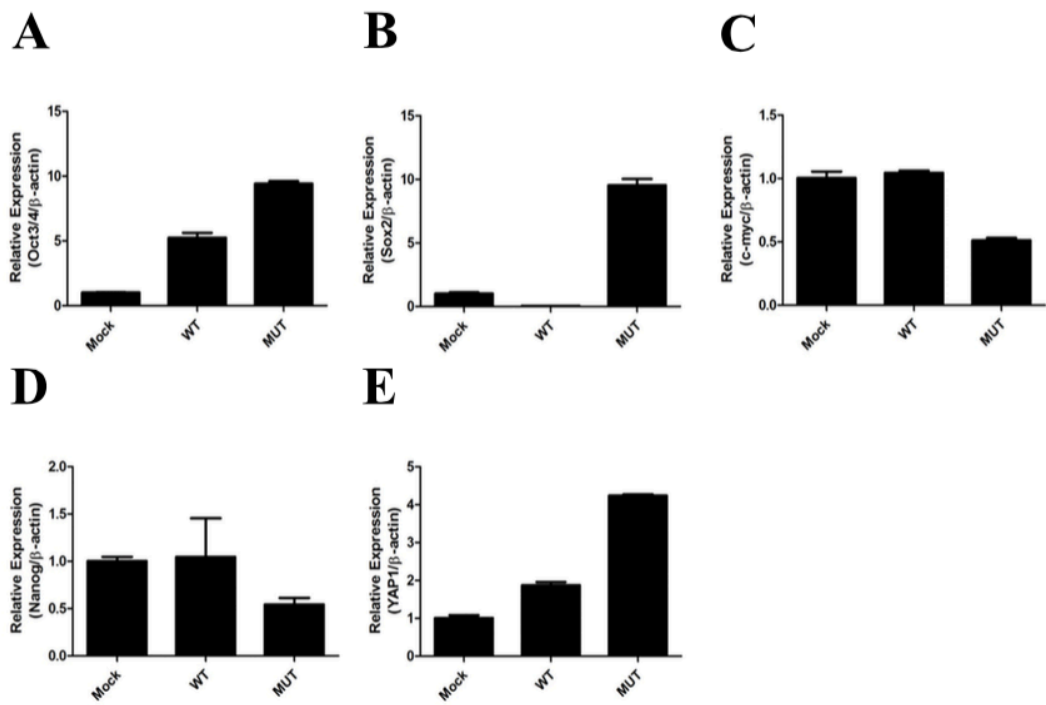


Figure 23 YAP1 R331W mutation increased relative expression level of Oct4 and

Sox2 *in vitro*.

YAP1 knockdown A549 cells were respectively transfected with 2 μ g vector control, 2 μ g YAP1 WT and 2 μ g YAP1 R331W plasmids for 48 hours and stable mix clones were selected by 400 μ g/ml of G418 and 2 μ g/ml of puromycin for 7 days. The relative expression level of four stemness markers Oct4 (A), Sox2 (B), C-myc (C) and Nanog (D) and YAP1 (E) were measured by using qRT-PCR.



Figure 24

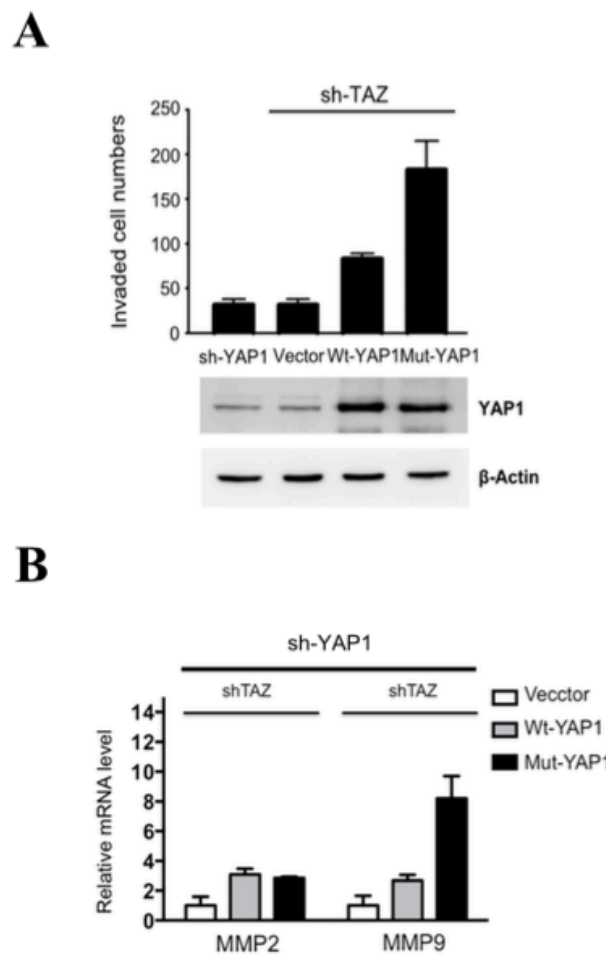


Figure 24 YAP1 R331W mutation significantly promoted invasiveness and enhanced MMP9 mRNA in TAZ knockdown cells.

A549 knockdown cells were infected with lentivirus expressing shTAZ vector and stable

mix clones were selected by puromycin for 7 days. YAP1/TAZ double knockdown A549

cells were respectively transfected with 2 μ g vector control, 2 μ g YAP1 WT and 2 μ g

YAP1 R331W plasmids for 48 hours and invasion assays were performed (A). Relative

expression level of MMP-2 and MMP-9 were determined by qRT-PCR (B).



Figure 25

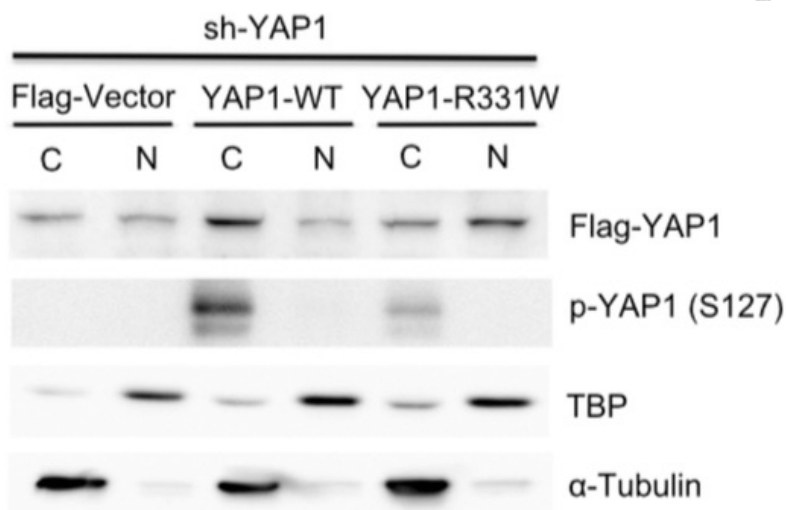


Figure 25 YAP1 R331W increased YAP1 nuclear accumulation and inhibited YAP1 S127 phosphorylation *in vitro*.

YAP1 knockdown A549 cells were respectively transfected with 2 μ g vector control, 2 μ g YAP1 WT and 2 μ g YAP1 R331W plasmids for 48 hours and extraction of cytoplasmic and nuclear proteins were conducted. The status of YAP1 nuclear accumulation and YAP1 S127 phosphorylation were detected by Western blot assays with flag antibody and p-YAP1 S127 antibody. β -actin served as an internal control.



Figure 26

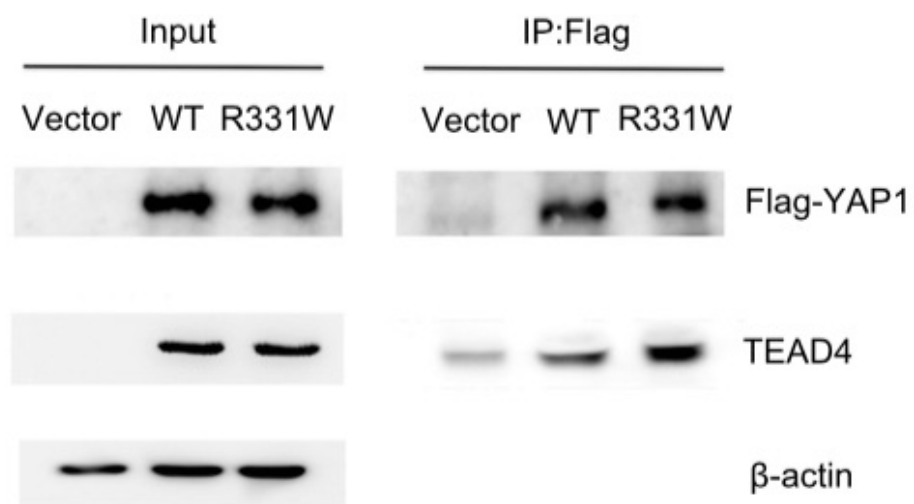


Figure 26 YAP1 R331W increased YAP1-TEAD4 interaction in lung

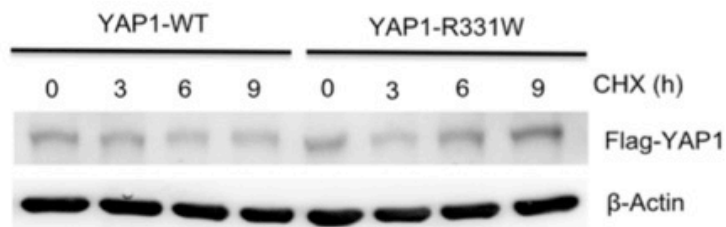
adenocarcinoma cells.

YAP1 knockdown cells were respectively transfected with 2 μ g Vector, 2 μ g flag-YAP1 WT and 2 μ g YAP1 R331W for 48 hours and lysates of transfected cells were performed with IP assay.



Figure 27

A



B

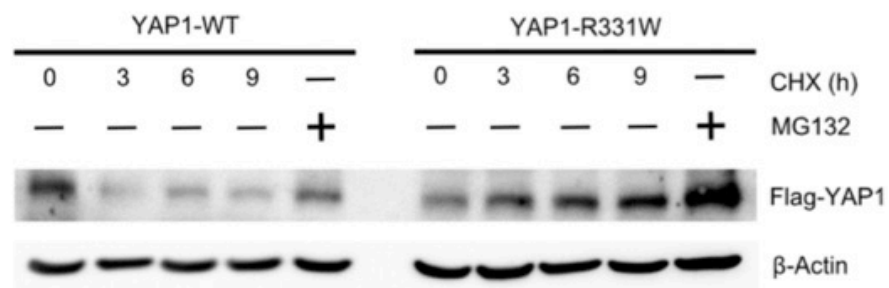


Figure 27 YAP1 R331W enhanced YAP1 protein stability.

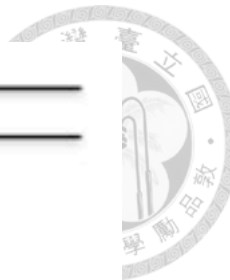
A, HEK293T cells were respectively transfected with 2μg Flag-YAP1 WT and 2μg Flag-YAP1 R331W plasmids for 48 hours and incubated with cycloheximide (CHX) for 0, 3, 6, 9 hours. YAP1 protein stability were determined by Western blot assay. B, HEK293T cells were respectively transfected with 2μg Flag-YAP1 WT and 2μg Flag-YAP1 R331W plasmids for 48 hours and incubated with CHX for 0, 3, 6, 9 hours and MG132 5 hours. YAP1 protein stability were determined by Western blot assay.



Table 1. Primer/Probe lists of experiments

Plasmid construction

Name	Sequence
HDAC53'UTR-F'	ACTAGTCGCCCCGGCCCCATC
HDAC5 3'UTR-R'	GTTTAAACGCCAGTGCCAGAAACAAGTT
HDAC5 3'UTR-Mut 1F'	TTCAGCTTAAAGGGGGGAA
HDAC5 3'UTR-Mut 1R'	CCCCCCTTAAAGCTGAAA
HDAC5 3'UTR-Mut 2F'	GATATGGAAAACAGTTAAGTATT
HDAC5 3'UTR-Mut 2R'	TACTTAACTGTTTCCATATCC
HDAC5 CDS-F'	AAGCTTATGAAtTCcCCCAACGAGT
HDAC5 CDS-R'	CTCGAGGCAAGtGCtGGCTCCTGCT
MMP-2-Promoter-F'	TTAACTCGAGCACACCCACCAAGACAAGCCT
MMP-2-Promoter-R'	TATAAGCTTAAGCCCCAGATGCGCAGCCT
MMP-9-Promoter-F'	TTAACTCGAGTTTCCCCATATCCTGCCCA
MMP-9-Promoter-R'	TATAAGCTTGGTGAGGGCAGAGGTGTCT
YAP1 CDS-Wt-F'	GAATTCATGGATCCGGGCAGCA
YAP1 CDS-Wt-R'	GCGGCCGCTAACCATGTAAGAAAG
YAP1 CDS-R331W-F'	GCAGGCAATGTGGAATATCAA
YAP1 CDS-R331W-R'	TTGATATTCCACATTGCCTGC



qRT-PCR (Taqman)

Name	Mature miRNA Sequence
has-miR-10a	UACCCUGUAGAUCCGAAUUUGUG
has-miR-10a*	CAAAUUCGUAUCUAGGGGAAUA
has-miR-146b-5p	UGAGAACUGAAUUCAUAGGCU
has-miR-149	UCUGGCUCCGUGUCUUCACUCCC
has-miR-335*	UUUUUCAUUAUUGCUCCUGACC
has-miR-598	GC GGUGAUCCCGAUGGGUGUGAGC

qRT-PCR (SYBR GREEN)

Name	Sequence
TBP-F'	CACGAACCACGGCACTGATT
TBP-R'	TTTTCTTGCTGCCAGTCTGGAC
HDAC5-F'	CATCGCTGAGAATGGCTTTACTG
HDAC5-R'	GACGTGTAGAGGCTGAACGGTT
MMP-1-F'	CTCGCTGGGAGCAAACACAT
MMP-1-R'	CTTGGCAAATCTGGCGTGTA
MMP-2-F'	CGATGTCGCCCAACATCA
MMP-2-R'	AGCCATAGAAGGTGTTCAAGGTATTG
MMP-9-F'	TGGCACCAACCACAACATCA
MMP-9-R'	GCCCCGGCAAGTCTT
MMP-10-F'	TGAGCCTAAGGTTGATGCTGTATT
MMP-10-R'	AACTGTGATGATCCACTGAAGAAGTAG
MMP-12-F'	CGCCTCTCTGCTGATGACATAC
MMP-12-R'	CAAGCGTTGGTTCTCTTTGG
YAP1-F'	GGC GCT CTT CAA CGC CGT CAT GAA C
YAP1-R'	CCT GTC GGG AGT GGG ATT T
TAZ-F'	CTTCAGCTTGGCAAGTGTGT
TAZ-R'	CCCTCATTCTGCTTGGAAAAA



Table 2. Six invasion-related miRNAs

microRNA	Fold Change
hsa-miR-10a	5.5967
hsa-miR-10a*	2.8199
hsa-miR-335*	2.4258
hsa-miR-149	2.1359
hsa-miR-598	0.2934
hsa-miR-146b-5p	0.4670

2 miRNAs (miR-598 and miR-146b-5p) showed a negative and 4 miRNAs (miR10a, miR-10a*, miR-335* and miR-149) showed a positive correlation between their miRNA expression and invasiveness.

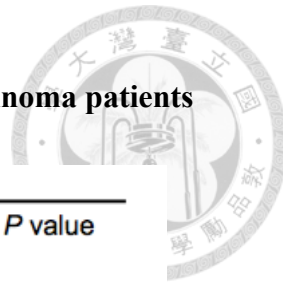


Table 3. Clinicopathological characteristics of 98 lung adenocarcinoma patients

Characteristic	All (N=98)	miR-10a*		P value
		Low-expression (N=49)	High-expression (N=49)	
Age (mean±SD)	66.18±11.75			0.88 ^a
Gender				1 ^b
-Female	44	22	22	
-Male	54	27	27	
Stage				0.30 ^b
-I	50	27	23	
-II	17	10	7	
-III	31	12	19	

^a Student t-test.

^b Fisher's exact test.

Table 4. Multivariate Cox regression analysis of the miR-10a* expression and survivals in 98 NSCLC patients



Gene	coefficient	p-value	Hazard Ratio	L95 CI	U95 CI
miR-10a-3p	0.165	4.37E-02	1.179	1.005	1.383
AGE	-0.005	6.93E-01	0.995	0.971	1.020
GENDER	0.521	9.05E-02	1.684	0.921	3.080
STAGE	0.686	2.50E-02	1.986	1.090	3.619

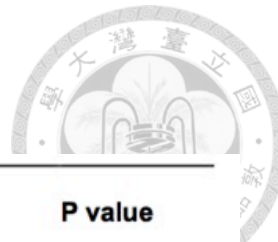


Table 5. MiR-10a*-altered pathways

Ranking	Pathway	P value
1 [#]	Cytoskeleton remodeling-Cytoskeleton remodeling	1.06e-12
2 [#]	Cytoskeleton remodeling-TGF, WNT and cytoskeletal remodeling	1.06e-12
3	Translation-Regulation of EIF4F activity	2.66e-9
4	Development-YAP/TAZ-mediated co-regulation of transcription	5.33e-8
5 [#]	Cell adhesion-Integrin-mediated cell adhesion and migration	6.70e-8
6 [#]	Cell adhesion-Chemokines and adhesion	7.53e-8
7	Immune response-Alternative complement pathway	8.99e-8
8 [#]	Cytoskeleton remodeling-Regulation of actin cytoskeleton by RhoGTPases	1.67e-7
9	Immune response-MIF-induced cell adhesion, migration and angiogenesis	1.69e-7
10	Cell cycle-Regulation of G1/S transition	1.87e-7

indicates invasion-related pathways

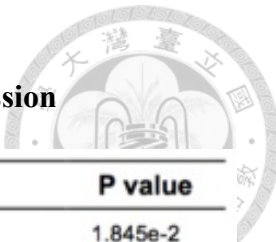


Table 6. Invasion related pathways altered by HDAC5 overexpression

Ranking	Pathway	P value
1	Cell adhesion_ECM remodeling	1.845e-2
2	Cytoskeleton remodeling_TGF, WNT and cytoskeletal remodeling	2.833e-1
3	Cell adhesion_Cell-matrix glycoconjugates	3.490e-1
4	Cell adhesion_PLAU signaling	3.811e-1
5	Cytoskeleton remodeling_Cytoskeleton remodeling	3.898e-1
6	Cell adhesion_Gap junctions	3.986e-1
7	Cell adhesion_Plasmin signaling	4.067e-1
8	Cell adhesion_Cadherin-mediated cell adhesion	4.286e-1
9	Development_BMP signaling	5.082e-1
10	Cell adhesion_PLAU signaling	5.481e-1
11	Cell adhesion_IL-8-dependent cell migration and adhesion	6.824e-1
12	Cell adhesion_Role of CDK5 in cell adhesion	8.693e-1
13	Cytoskeleton remodeling_Fibronectin-binding integrins in cell motility	9.011e-1
14	Cytoskeleton remodeling_ACM3 and ACM4 in keratinocyte migration	9.907e-1
15	Cell adhesion_Alpha-4 integrins in cell migration and adhesion	9.961e-1

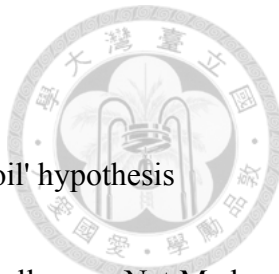
Table 7. Potential transcription factors involved in HDAC5-mediated regulation of MMP-2 and MMP-9



MMP-2		MMP-9	
TF	Fold change	TF	Fold change
AP1	0.37	AP1	0.37
ATF3	2.43	NFKB1	1.37
GATA2	1.36	AR	—
SRF	—	YY1	—
YY1	—	RELA	—
RELA	—	TBP	—
TBP	—	SRY	—
CEBPA	—	SP1	—
MEF2A	—	STAT4	—
ELF1	—		
ELK1	—		
FOXP3	—		
SRY	—		
P53	—		
HOXD9	—		
POU2F2	—		
SP1	—		
PAX5	—		
POU2F1	—		
GATA1	—		
GATA3	—		
STAT4	—		
XBP1	—		

Bold character indicates the differentially expressed TFs found in both MMP regulations

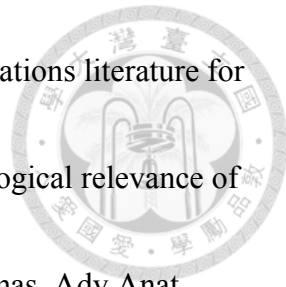
References



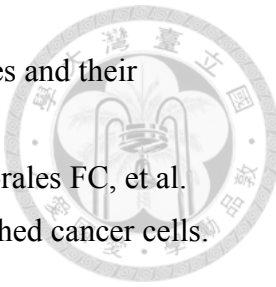
1. Fidler IJ. The pathogenesis of cancer metastasis: the 'seed and soil' hypothesis revisited. *Nat Rev Cancer*. 2003;3:453-8.
2. Steeg PS. Tumor metastasis: mechanistic insights and clinical challenges. *Nat Med*. 2006;12:895-904.
3. Gupta GP, Massague J. Cancer metastasis: building a framework. *Cell*. 2006;127:679-95.
4. Schroeder A, Heller DA, Winslow MM, Dahlman JE, Pratt GW, Langer R, et al. Treating metastatic cancer with nanotechnology. *Nat Rev Cancer*. 2012;12:39-50.
5. Weiss L. Metastasis of cancer: a conceptual history from antiquity to the 1990s. *Cancer Metastasis Rev*. 2000;19:I-XI, 193-383.
6. Howlader N NA, Krapcho M, Miller D, Bishop K, Altekruse SF, Kosary CL, Yu M, Ruhl J, Tatalovich Z, Mariotto A, Lewis DR, Chen HS, Feuer EJ, Cronin KA (eds).
7. Shiraishi K, Kunitoh H, Daigo Y, Takahashi A, Goto K, Sakamoto H, et al. A genome-wide association study identifies two new susceptibility loci for lung adenocarcinoma in the Japanese population. *Nature genetics*. 2012;44:900-3.
8. Lu J, Getz G, Miska EA, Alvarez-Saavedra E, Lamb J, Peck D, et al. MicroRNA expression profiles classify human cancers. *Nature*. 2005;435:834-8.
9. Sun W, Julie Li YS, Huang HD, Shyy JY, Chien S. microRNA: a master regulator of cellular processes for bioengineering systems. *Annu Rev Biomed Eng*. 2010;12:1-27.
10. He L, Thomson JM, Hemann MT, Hernando-Monge E, Mu D, Goodson S, et al. A microRNA polycistron as a potential human oncogene. *Nature*. 2005;435:828-33.
11. Pencheva N, Tavazoie SF. Control of metastatic progression by microRNA regulatory networks. *Nat Cell Biol*. 2013;15:546-54.
12. Ma L, Teruya-Feldstein J, Weinberg RA. Tumour invasion and metastasis initiated by microRNA-10b in breast cancer. *Nature*. 2007;449:682-8.
13. Liu C, Kelnar K, Liu B, Chen X, Calhoun-Davis T, Li H, et al. The microRNA miR-34a inhibits prostate cancer stem cells and metastasis by directly repressing CD44. *Nat Med*. 2011;17:211-5.
14. Yang S, Li Y, Gao J, Zhang T, Li S, Luo A, et al. MicroRNA-34 suppresses breast cancer invasion and metastasis by directly targeting Fra-1. *Oncogene*. 2013;32:4294-303.
15. Siemens H, Jackstadt R, Hunten S, Kaller M, Menssen A, Gotz U, et al. miR-34

and SNAIL form a double-negative feedback loop to regulate epithelial-mesenchymal transitions. *Cell Cycle*. 2011;10:4256-71.

16. Waldman SA, Terzic A. A study of microRNAs in silico and in vivo: diagnostic and therapeutic applications in cancer. *FEBS J*. 2009;276:2157-64.
17. Roth SY, Denu JM, Allis CD. Histone acetyltransferases. *Annual review of biochemistry*. 2001;70:81-120.
18. Bolden JE, Peart MJ, Johnstone RW. Anticancer activities of histone deacetylase inhibitors. *Nat Rev Drug Discov*. 2006;5:769-84.
19. Renthal W, Maze I, Krishnan V, Covington HE, 3rd, Xiao G, Kumar A, et al. Histone deacetylase 5 epigenetically controls behavioral adaptations to chronic emotional stimuli. *Neuron*. 2007;56:517-29.
20. Long X, Creemers EE, Wang DZ, Olson EN, Miano JM. Myocardin is a bifunctional switch for smooth versus skeletal muscle differentiation. *Proc Natl Acad Sci U S A*. 2007;104:16570-5.
21. McKinsey TA, Zhang CL, Lu J, Olson EN. Signal-dependent nuclear export of a histone deacetylase regulates muscle differentiation. *Nature*. 2000;408:106-11.
22. McKinsey TA, Zhang CL, Olson EN. Activation of the myocyte enhancer factor-2 transcription factor by calcium/calmodulin-dependent protein kinase-stimulated binding of 14-3-3 to histone deacetylase 5. *Proc Natl Acad Sci U S A*. 2000;97:14400-5.
23. Osada H, Tatematsu Y, Saito H, Yatabe Y, Mitsudomi T, Takahashi T. Reduced expression of class II histone deacetylase genes is associated with poor prognosis in lung cancer patients. *Int J Cancer*. 2004;112:26-32.
24. Scanlan MJ, Welt S, Gordon CM, Chen YT, Gure AO, Stockert E, et al. Cancer-related serological recognition of human colon cancer: identification of potential diagnostic and immunotherapeutic targets. *Cancer research*. 2002;62:4041-7.
25. Bradbury CA, Khanim FL, Hayden R, Bunce CM, White DA, Drayson MT, et al. Histone deacetylases in acute myeloid leukaemia show a distinctive pattern of expression that changes selectively in response to deacetylase inhibitors. *Leukemia*. 2005;19:1751-9.
26. Milde T, Oehme I, Korshunov A, Kopp-Schneider A, Remke M, Northcott P, et al. HDAC5 and HDAC9 in medulloblastoma: novel markers for risk stratification and role in tumor cell growth. *Clin Cancer Res*. 2010;16:3240-52.
27. Pon JR, Marra MA. Driver and passenger mutations in cancer. *Annu Rev Pathol*. 2015;10:25-50.



28. Kern SE, Winter JM. Elegance, silence and nonsense in the mutations literature for solid tumors. *Cancer Biol Ther*. 2006;5:349-59.
29. Pakneshan S, Salajegheh A, Smith RA, Lam AK. Clinicopathological relevance of BRAF mutations in human cancer. *Pathology*. 2013;45:346-56.
30. Slack GW, Gascoyne RD. MYC and aggressive B-cell lymphomas. *Adv Anat Pathol*. 2011;18:219-28.
31. Ciriello G, Miller ML, Aksoy BA, Senbabaoglu Y, Schultz N, Sander C. Emerging landscape of oncogenic signatures across human cancers. *Nature genetics*. 2013;45:1127-33.
32. Sudol M. Yes-associated protein (YAP65) is a proline-rich phosphoprotein that binds to the SH3 domain of the Yes proto-oncogene product. *Oncogene*. 1994;9:2145-52.
33. Camargo FD, Gokhale S, Johnnidis JB, Fu D, Bell GW, Jaenisch R, et al. YAP1 increases organ size and expands undifferentiated progenitor cells. *Curr Biol*. 2007;17:2054-60.
34. Cao X, Pfaff SL, Gage FH. YAP regulates neural progenitor cell number via the TEA domain transcription factor. *Genes Dev*. 2008;22:3320-34.
35. Lian I, Kim J, Okazawa H, Zhao J, Zhao B, Yu J, et al. The role of YAP transcription coactivator in regulating stem cell self-renewal and differentiation. *Genes Dev*. 2010;24:1106-18.
36. Liu R, Huang S, Lei Y, Zhang T, Wang K, Liu B, et al. FGF8 promotes colorectal cancer growth and metastasis by activating YAP1. *Oncotarget*. 2015;6:935-52.
37. Zender L, Spector MS, Xue W, Flemming P, Cordon-Cardo C, Silke J, et al. Identification and validation of oncogenes in liver cancer using an integrative oncogenomic approach. *Cell*. 2006;125:1253-67.
38. Chen HY, Yu SL, Ho BC, Su KY, Hsu YC, Chang CS, et al. R331W Missense Mutation of Oncogene YAP1 Is a Germline Risk Allele for Lung Adenocarcinoma With Medical Actionability. *J Clin Oncol*. 2015;33:2303-10.
39. Yu SL, Chen HY, Chang GC, Chen CY, Chen HW, Singh S, et al. MicroRNA signature predicts survival and relapse in lung cancer. *Cancer Cell*. 2008;13:48-57.
40. Hsu YC, Yuan S, Chen HY, Yu SL, Liu CH, Hsu PY, et al. A four-gene signature from NCI-60 cell line for survival prediction in non-small cell lung cancer. *Clin Cancer Res*. 2009;15:7309-15.
41. Miranda KC, Huynh T, Tay Y, Ang YS, Tam WL, Thomson AM, et al. A



pattern-based method for the identification of MicroRNA binding sites and their corresponding heteroduplexes. *Cell*. 2006;126:1203-17.

42. Muranen T, Selfors LM, Worster DT, Iwanicki MP, Song L, Morales FC, et al. Inhibition of PI3K/mTOR leads to adaptive resistance in matrix-attached cancer cells. *Cancer Cell*. 2012;21:227-39.

43. Moskot M, Jakobkiewicz-Banecka J, Smolinska E, Piotrowska E, Wegrzyn G, Gabig-Ciminska M. Effects of flavonoids on expression of genes involved in cell cycle regulation and DNA replication in human fibroblasts. *Molecular and cellular biochemistry*. 2015;407:97-109.

44. Wang SP, Wang WL, Chang YL, Wu CT, Chao YC, Kao SH, et al. p53 controls cancer cell invasion by inducing the MDM2-mediated degradation of Slug. *Nat Cell Biol*. 2009;11:694-704.

45. Chen CC, Chen HY, Su KY, Hong QS, Yan BS, Chen CH, et al. Shisa3 is associated with prolonged survival through promoting beta-catenin degradation in lung cancer. *Am J Respir Crit Care Med*. 2014;190:433-44.

46. Chen CH, Chang WH, Su KY, Ku WH, Chang GC, Hong QS, et al. HLJ1 is an endogenous Src inhibitor suppressing cancer progression through dual mechanisms. *Oncogene*. 2016.

47. Egeblad M, Werb Z. New functions for the matrix metalloproteinases in cancer progression. *Nat Rev Cancer*. 2002;2:161-74.

48. Messeguer X, Escudero R, Farre D, Nunez O, Martinez J, Alba MM. PROMO: detection of known transcription regulatory elements using species-tailored searches. *Bioinformatics*. 2002;18:333-4.

49. Mathelier A, Zhao X, Zhang AW, Parcy F, Worsley-Hunt R, Arenillas DJ, et al. JASPAR 2014: an extensively expanded and updated open-access database of transcription factor binding profiles. *Nucleic acids research*. 2014;42:D142-7.

50. Bian J, Sun Y. Transcriptional activation by p53 of the human type IV collagenase (gelatinase A or matrix metalloproteinase 2) promoter. *Mol Cell Biol*. 1997;17:6330-8.

51. Shin SY, Kim JH, Baker A, Lim Y, Lee YH. Transcription factor Egr-1 is essential for maximal matrix metalloproteinase-9 transcription by tumor necrosis factor alpha. *Mol Cancer Res*. 2010;8:507-19.

52. Kanai F, Marignani PA, Sarbassova D, Yagi R, Hall RA, Donowitz M, et al. TAZ: a novel transcriptional co-activator regulated by interactions with 14-3-3 and PDZ domain proteins. *EMBO J*. 2000;19:6778-91.

53. Hsu YC, Chen HY, Yuan S, Yu SL, Lin CH, Wu G, et al. Genome-wide analysis of three-way interplay among gene expression, cancer cell invasion and anti-cancer compound sensitivity. *BMC Med.* 2013;11:106.

54. Ujifuku K, Mitsutake N, Takakura S, Matsuse M, Saenko V, Suzuki K, et al. miR-195, miR-455-3p and miR-10a(*) are implicated in acquired temozolomide resistance in glioblastoma multiforme cells. *Cancer letters.* 2010;296:241-8.

55. Zhu S, Deng S, Ma Q, Zhang T, Jia C, Zhuo D, et al. MicroRNA-10A* and MicroRNA-21 modulate endothelial progenitor cell senescence via suppressing high-mobility group A2. *Circ Res.* 2013;112:152-64.

56. Tong L, Lin L, Wu S, Guo Z, Wang T, Qin Y, et al. MiR-10a* up-regulates coxsackievirus B3 biosynthesis by targeting the 3D-coding sequence. *Nucleic acids research.* 2013;41:3760-71.

57. Glazkova MA, Seto E. Histone deacetylases and cancer. *Oncogene.* 2007;26:5420-32.

58. Barlesi F, Giaccone G, Gallegos-Ruiz MI, Loundou A, Span SW, Lefevre P, et al. Global histone modifications predict prognosis of resected non small-cell lung cancer. *J Clin Oncol.* 2007;25:4358-64.

59. Bai X, Wu L, Liang T, Liu Z, Li J, Li D, et al. Overexpression of myocyte enhancer factor 2 and histone hyperacetylation in hepatocellular carcinoma. *J Cancer Res Clin Oncol.* 2008;134:83-91.

60. Mohamed MA, Greif PA, Diamond J, Sharaf O, Maxwell P, Montironi R, et al. Epigenetic events, remodelling enzymes and their relationship to chromatin organization in prostatic intraepithelial neoplasia and prostatic adenocarcinoma. *BJU Int.* 2007;99:908-15.

61. Shahbazian MD, Grunstein M. Functions of site-specific histone acetylation and deacetylation. *Annual review of biochemistry.* 2007;76:75-100.

62. Ceccacci E, Minucci S. Inhibition of histone deacetylases in cancer therapy: lessons from leukaemia. *Br J Cancer.* 2016;114:605-11.

63. Kim HJ, Bae SC. Histone deacetylase inhibitors: molecular mechanisms of action and clinical trials as anti-cancer drugs. *Am J Transl Res.* 2011;3:166-79.

64. Pulukuri SM, Gorantla B, Rao JS. Inhibition of histone deacetylase activity promotes invasion of human cancer cells through activation of urokinase plasminogen activator. *The Journal of biological chemistry.* 2007;282:35594-603.

65. Lin KT, Wang YW, Chen CT, Ho CM, Su WH, Jou YS. HDAC inhibitors

augmented cell migration and metastasis through induction of PKCs leading to identification of low toxicity modalities for combination cancer therapy. *Clin Cancer Res.* 2012;18:4691-701.

66. Qin H, Sun Y, Benveniste EN. The transcription factors Sp1, Sp3, and AP-2 are required for constitutive matrix metalloproteinase-2 gene expression in astrogloma cells. *The Journal of biological chemistry.* 1999;274:29130-7.
67. Chung TW, Lee YC, Kim CH. Hepatitis B viral HBx induces matrix metalloproteinase-9 gene expression through activation of ERK and PI-3K/AKT pathways: involvement of invasive potential. *FASEB J.* 2004;18:1123-5.
68. Song C, Zhu S, Wu C, Kang J. Histone deacetylase (HDAC) 10 suppresses cervical cancer metastasis through inhibition of matrix metalloproteinase (MMP) 2 and 9 expression. *The Journal of biological chemistry.* 2013;288:28021-33.
69. Wang XX, Cheng Q, Zhang SN, Qian HY, Wu JX, Tian H, et al. PAK5-Egr1-MMP2 signaling controls the migration and invasion in breast cancer cell. *Tumour biology : the journal of the International Society for Oncodevelopmental Biology and Medicine.* 2013;34:2721-9.
70. Yu G, Li H, Wang X, Wu T, Zhu J, Huang S, et al. MicroRNA-19a targets tissue factor to inhibit colon cancer cells migration and invasion. *Molecular and cellular biochemistry.* 2013;380:239-47.
71. Legrand C, Polette M, Tournier JM, de Bentzmann S, Huet E, Monteau M, et al. uPA/plasmin system-mediated MMP-9 activation is implicated in bronchial epithelial cell migration. *Experimental cell research.* 2001;264:326-36.
72. del Barco Barrantes I, Nebreda AR. Roles of p38 MAPKs in invasion and metastasis. *Biochemical Society transactions.* 2012;40:79-84.
73. Simon C, Goepfert H, Boyd D. Inhibition of the p38 mitogen-activated protein kinase by SB 203580 blocks PMA-induced Mr 92,000 type IV collagenase secretion and in vitro invasion. *Cancer research.* 1998;58:1135-9.
74. Zhao B, Wei X, Li W, Udan RS, Yang Q, Kim J, et al. Inactivation of YAP oncoprotein by the Hippo pathway is involved in cell contact inhibition and tissue growth control. *Genes Dev.* 2007;21:2747-61.
75. Zhao B, Li L, Tumaneng K, Wang CY, Guan KL. A coordinated phosphorylation by Lats and CK1 regulates YAP stability through SCF(beta-TRCP). *Genes Dev.* 2010;24:72-85.
76. Hanahan D, Weinberg RA. Hallmarks of cancer: the next generation. *Cell.*

2011;144:646-74.

